PHYSICAL REVIEW D **86,** 054502 (2012)

Wilson loops to 20th order numerical stochastic perturbation theory

R. Horsley,[1] G. Hotzel,[2,*] E.-M. Ilgenfritz,[3,4] R. Millo,[5] H. Perlt,[2] P. E. L. Rakow,[5] Y. Nakamura,[6] G. Schierholz,[7] and A. Schiller[2]

[1]*School of Physics, University of Edinburgh, Edinburgh EH9 3JZ, United Kingdom*
[2]*Institut für Theoretische Physik, Universität Leipzig, D-04109 Leipzig, Germany*
[3]*Institut für Physik, Humboldt-Universität zu Berlin, D-12489 Berlin, Germany*
[4]*Joint Institute for Nuclear Research, VBLHEP, 141980 Dubna, Russia*
[5]*Theoretical Physics Division, Department of Mathematical Sciences, University of Liverpool, Liverpool L69 3BX, United Kingdom*
[6]*RIKEN Advanced Institute for Computational Science, Kobe, Hyogo 650-0047, Japan*
[7]*Deutsches Elektronen-Synchrotron DESY, D-22603 Hamburg, Germany*

(Received 23 May 2012; published 6 September 2012)

We calculate perturbative contributions of Wilson loops of various sizes up to order 20 in $SU(3)$ pure lattice gauge theory at different lattice sizes for the Wilson gauge action using the technique of numerical stochastic perturbation theory. This allows us to investigate the perturbative series for various Wilson loops at high orders of the perturbation theory. We observe differences in the behavior of the series as a function of the loop order n. Up to $n = 20$ we do not find evidence for the factorial growth of the expansion coefficients often assumed to characterize an asymptotic series. Based on the actually observed behavior we sum the series in a model parametrized by hypergeometric functions. For Wilson loops of moderate sizes the summed series in boosted perturbation theory reach stable plateaus for moderate perturbative order already. The coefficients in the boosted series become much more stable in the result of smoothing the coefficients of the original series effected by the hypergeometric model. We introduce generalized ratios of Wilson loops of different sizes. Together with the corresponding Wilson loops from standard Monte Carlo measurements they enable us to assess their nonperturbative parts.

DOI: 10.1103/PhysRevD.86.054502 PACS numbers: 11.15.Ha, 12.38.Aw, 12.38.Cy, 12.38.Gc

I. INTRODUCTION

Since the nonperturbative gluon condensate has been introduced by Shifman, Vainshtein and Zakharov [1] there have been many attempts to obtain reliable numerical values for this quantity. It has become clear that lattice gauge theory provides a promising tool to calculate the gluon condensate from first principles using Wilson loops W_{NM} of various sizes $N \times M$. The perturbative expansion of the Wilson loop—which does not depend on an external scale—is especially simple since it cannot depend on logarithms. In Refs. [2,3] the plaquette was used whereas larger Wilson loops have been investigated in Refs. [4,5]. In all cases it turned out that knowledge—as precisely as possible—of the large order perturbative tail of the Wilson loops is crucial. In the last decade, the application of the numerical stochastic perturbation theory (NSPT) [6] has pushed the perturbative order of the plaquette up to order $n = 10$ [7] and even $n = 16$ [8].

Apart from the desired evaluation of the gluon condensate, there is a general interest in the behavior of the perturbative series in QCD (for an investigation see Ref. [9]). In the perturbation theory, observables can be written as a series of the form

$$\mathcal{O} \sim \sum_n c_n \lambda^n, \tag{1}$$

where λ denotes some generic coupling, e.g., α_s. It is generally believed that these series are asymptotic ones, and it is often assumed that for large n the leading growth of the coefficients c_n can be parametrized as [10]

$$c_n \sim C_1 (C_2)^n \Gamma(n + C_3), \tag{2}$$

with some constants C_1, C_2, C_3, i.e., they show a factorial behavior.

Using the technique of NSPT one can reach loop orders of the perturbation theory where a possible set-in of this assumed behavior becomes testable. In Ref. [11] Narison and Zakharov discussed the difference between short and long perturbative series and the impact on the determination of the gluon condensate.

In this paper we present perturbative calculations of Wilson loops in NSPT for the Wilson gauge action (with $\beta = 6/g^2$)

$$S_W[U] = \beta \sum_P \left[1 - \frac{1}{6} \mathrm{Tr}(U_P + U_P^\dagger) \right], \tag{3}$$

up to order $n = 20$ for lattice sizes L^4 with $L = 4, 6, 8, 12$. The computations for $L = 12$ were performed on a NEC SX-9 computer at the Research Center for Nuclear Physics, Osaka University, all the rest on Linux/HP clusters at Leipzig University.

*Present address: Institut für Physik, Humboldt-Universität zu Berlin, D-12489 Berlin, Germany

The paper is organized as follows. In Sec. II we explain how the loop order expansion of Wilson loops has been obtained in NSPT. In Sec. III we discuss a model which allows us to sum up completely the obtained Wilson loops series on finite lattices. As an alternative we apply boosted perturbation theory: due to a rearrangement of the series one obtains good convergence of the sum up to relatively low loop order already. These results are used to estimate the gluon condensate in Sec. IV. Finally we draw our conclusions.

Some preliminary results have been presented in recent lattice proceedings [12,13]. In the present work we give the computational details of the Langevin calculation for the final statistics reached and significantly extend the analysis part using boosting and series summation as well as adding new aspects to the analysis of Wilson loops of moderate size.

II. NSPT AND WILSON LOOPS UP TO 20 LOOPS

A. The strategy of NSPT

Numerical stochastic perturbation theory—based on stochastic quantization [14]—allows perturbative calculations on finite lattices up to finite but high loop order n, unrivaled by the standard diagrammatic approach in lattice perturbation theory. Practical limits are set only by computer time, storage limitations and machine precision. For instance, in order to calculate in the n-loop order in the simplest realization of NSPT in the Euler scheme, one has to keep simultaneously links corresponding to roughly $2n$ gauge field configurations for a given lattice size. If one wants to keep for practical reasons also the gauge fields (vector potentials) besides the gauge field links themselves, the storage requirement is even doubled. In addition, the computer time of the Langevin simulation scales quite severely; we found it roughly goes like n^3.

The algorithm of NSPT has been introduced and discussed in detail in Refs. [6,15]. For convenience, we will repeat the main points for the pure $SU(3)$ lattice gauge theory. The stochastic evolution of the gauge field links $U_{x,\mu}$, located at the link between lattice sites x and $x+\hat{\mu}$, occurs in an additional "Langevin time" τ. This process is described by the Langevin equation

$$\frac{\partial}{\partial\tau}U_{x,\mu}(\tau;\eta) = \mathrm{i}\{\nabla_{x,\mu}S_W[U] - \eta_{x,\mu}(\tau)\}U_{x,\mu}(\tau;\eta). \quad (4)$$

The so-called drift term is given by the variation of the Euclidean gauge action $S_W[U]$: it is written in terms of the left Lie derivative $\nabla_{x,\mu}$ which keeps the links in the $SU(3)$ group manifold. The process is made stochastic by additive white noise $\eta_{x,\mu}(\tau)$. In the limit of large τ the distribution of subsequent, simultaneous gauge link fields converges to the Gibbs measure $P[U] \propto \exp(-S_W[U])$.

As in any numerical approach one needs to discretize the Langevin time as a sequence $\tau \to k\epsilon$, with running step number k. It is known that, in order to extract correct equilibrium physics, one needs to perform the double extrapolation $k \to \infty$ and $\epsilon \to 0$, the latter in order not to violate detailed balance. For the numerical solution of the Langevin equation we adhere to a particular version of the Euler scheme that guarantees all the link matrices $U_{x,\mu} \in SU(3)$ to stay in the group manifold:

$$U_{x,\mu}(k+1;\eta) = \exp(\mathrm{i}F_{x,\mu}[U,\eta])U_{x,\mu}(k;\eta), \quad (5)$$

with the force term for the update of the gauge links $U_{x,\mu}(k;\eta)$ in the form

$$F_{x,\mu}[U,\eta] = \epsilon\nabla_{x,\mu}S_W[U] + \sqrt{\epsilon}\eta_{x,\mu}, \quad (6)$$

η being a traceless 3×3 noise matrix. In case of the Wilson gauge action that force term takes the form

$$F_{x,\mu} = \frac{\beta\epsilon}{12}\sum_{U_P\supset U_{x,\mu}}\left[(U_P - U_P^\dagger) - \frac{1}{3}\mathrm{Tr}(U_P - U_P^\dagger)\mathbb{1}\right] + \sqrt{\epsilon}\eta_{x,\mu}. \quad (7)$$

We expand each link matrix at any time step in the bare coupling constant g around the trivial vacuum $U_{x,\mu} = \mathbb{1}$. Since $\beta = 6/g^2$, the expansion reads

$$U_{x,\mu}(k;\eta) \to \mathbb{1} + \sum_{m\geq 1}\beta^{-m/2}U_{x,\mu}^{(m)}(k;\eta). \quad (8)$$

If one rescales the time step to $\varepsilon = \beta\epsilon$, the expansion (8) converts the Langevin equation, Eq. (5), into a system of simultaneous updates in terms of the expansion coefficients of $U_{x,\mu}^{(m)}(k;\eta)$ and of similar expansion coefficients for the force $F_{x,\mu}$ in (7), but free of adjustable constants. While the random noise η enters only the lowest order equation, higher orders are rendered stochastic by the noise propagating from lower to higher order terms. The system is usually truncated according to the maximal order of the perturbative gauge link fields one is interested in.

For NSPT it is indispensable to perform stochastic gauge fixing by using a variant of gauge transformations,

$$U_{x,\mu}^G = G_x U_{x,\mu} G_{x+\hat{\mu}}^\dagger, \quad (9)$$

with G_x derived from the Landau gauge and expanded in powers of $1/\sqrt{\beta} \sim g$. A convenient solution for the gauge transformation G comes with the choice

$$G_x = \exp\left\{-\alpha\sum_\nu\left(\frac{A_{x+\hat{\nu}/2,\nu} - A_{x-\hat{\nu}/2,\nu}}{a}\right)\right\}, \quad (10)$$

where the series variant of the expression has to be taken. Here the (anti-Hermitian) vector potential $A_{x+\hat{\mu}/2,\mu}$ is related to the link matrices $U_{x,\mu}$ via

$$A_{x+\hat{\mu}/2,\mu} = \log U_{x,\mu}, \quad (11)$$

and an expansion similar to (8) taking values in the algebra $su(3)$ is applied for the potential.

The need for stochastic gauge fixing comes from the fact that the diffusion of the longitudinal component of the A_μ

fields is unbounded and hence their norms would diverge in the course of the stochastic process. Although gauge-invariant quantities are in principle not affected by these divergences, the performance eventually runs into trouble due to loss of accuracy. It turns out that one step of (9) using (10) alternating with the Langevin step (5) is sufficient to keep fluctuations under control, if α is chosen of order $\alpha \sim \varepsilon$.

The influence of zero modes of the gluon field on the performance of the Langevin process has been critically discussed in Ref. [15]. Since zero modes (constant modes) of the gauge fields do not contribute to the discretized divergence present in (10), they would not be subtracted by performing the gauge transformation. We take the simplest prescription of subtracting zero modes at every order by hand. This completes the specification how NSPT is used in our calculations.

Let us remark that, whenever we speak about contributions of some order to an observable constructed out of links, this has to be understood in the sense of an expansion,

$$\langle \mathcal{O} \rangle \to \sum_{m \geq 0} \beta^{-m/2} \langle \mathcal{O}^{(m)} \rangle, \tag{12}$$

and the expansion coefficients $\langle \mathcal{O}^{(m)} \rangle$ are extracted out of the expanded right-hand side of (8) by comparing coefficients of equal powers $\beta^{-m/2}$ (or g^m). In the notation of (12) even integers m correspond to genuine loop contributions (with loop order $m/2$). In the computer implementation of NSPT we practically measure observables for various small but finite values of ε. The final result is then obtained by performing the extrapolation to $\varepsilon \to 0$ for the observables in each loop order.

B. NSPT results for Wilson loops in high order perturbation theory

In lattice gauge theory the Wilson loop as a gauge invariant quantity built only out of gauge field links is defined as the trace of a product of link fields along a closed path C,

$$W_C[U] = \frac{1}{3} \mathrm{Tr} \prod_{(x,\mu) \in C} U_{x,\mu}. \tag{13}$$

Having at our disposal the expansion of the links (at finite Langevin step size) close to the trivial vacuum $U^{(0)}_{x,\mu} \equiv \mathbb{1}$ to all orders in $g \propto 1/\sqrt{\beta}$,[1]

$$U_{x,\mu} \equiv \sum_{m \geq 0} U^{(m)}_{x,\mu} g^m, \tag{14}$$

we construct perturbative Wilson loops within a given "Langevin configuration" (at fixed Langevin time). Inserting the expansion (14) for the links in (13) we collect terms of equal power in g on the right-hand side and identify these with the n-th loop order contribution $W^{(n)}_C$ on the left-hand side,

$$\sum_{n=0,1/2,1,3/2,\ldots} W^{(n)}_C g^{2n} = \frac{1}{3} \mathrm{Tr} \prod_{(x,\mu) \in C} \left[\sum_{m_{x,\mu} \geq 0} U^{(m_{x,\mu})}_{x,\mu} g^{m_{x,\mu}} \right]. \tag{15}$$

The final result involves averaging over different configurations obtained during the Langevin evolution and the extrapolation to $\varepsilon \to 0$.

Here we consider rectangular Wilson loops C of size $N \times M$, where we restrict the maximal side length of the Wilson loop to half of the lattice size $L/2$ for a lattice L^4. Therefore, we identify the general perturbative loop order expansion of the Wilson loop W_{NM} in terms of the bare lattice coupling g as

$$W_{NM} = \sum_{n=0,1/2,1,3/2,\ldots} W^{(n)}_{NM} g^{2n}, \tag{16}$$

with the Wilson loop expansion coefficients $W^{(n)}_{NM}$ ($W^{(0)}_{NM} \equiv 1$). The integer powers $n = 1, 2, \ldots$ in the series (16) denote the perturbative loop orders as in the diagrammatic perturbation theory.

In addition, following (15) we measure analogues of the loop coefficients $W^{(n)}_{NM}$ also for half-integer $n = 3/2, 5/2, \ldots$. (Due to the color trace the coefficient with $n = 1/2$ is identically equal to zero.) Averages over coefficients with those half-integers—which describe nonloop contributions—should vanish numerically after averaging over a sufficient number of measurements and define some level of "noise" for finite statistics to be compared to the *loop* contributions. While higher loop order contributions decrease fast with the loop number, the noise does not decrease sufficiently fast, staying near zero. Therefore, we adopt here the criterion that we can take the expansion coefficients for a given loop order n for granted ("reliable") only if they can be clearly distinguished numerically from the noisy results for adjacent nonloop contributions of orders $n - 1/2$ and $n + 1/2$. We do not rule out the possibility of an extrapolation to zero Langevin step size crossing in a systematic way the noise region near zero from a positive/negative coefficient at large ε to a negative/positive coefficient at smallest ε. The coefficient extrapolated to $\varepsilon = 0$ might be as small as the noise of the adjacent nonloop contributions.

Let us add some details of the perturbative Langevin simulation: Instead of having one link configuration as in usual Monte Carlo studies, we have to handle 40 link configurations building our "perturbative" configuration for each g order to reach loop order 20 at each Langevin step. So, unavoidably, the different orders in g are

[1]From now on we use as expansion parameter the gauge coupling g, using the same notation for the coefficients $U^{(m)}_{x,\mu}$.

correlated, since we have to use a correlated system of Langevin equations for each order.

Any simulation for a chosen Langevin step size ε starts from a link configuration, where the zeroth order in g of the expanded links is put equal to one (and remains so during all the evolution), whereas all nonzero orders in g are set initially to zero (a ''cold'' start). So any loop contribution is by construction vanishing at the beginning. Starting from here with the Langevin process including the noise term, the nonzero g orders of the links iteratively obtain nonzero values at each link position starting from the lowest order in g. Therefore, the highest order in g needs the highest minimal number of Langevin steps to reach equilibrium. With decreasing step size ε that minimal number also increases.

As a criterion to reach the equilibrium of the Langevin process, we studied the behavior of the perturbative plaquette. By monitoring the highest order of the plaquette at the lowest chosen step size $\varepsilon = 0.01$, we observed that equilibrium is reached after roughly 2000 Langevin steps. To be on the safe side we have discarded the first 5000 Langevin steps after a cold start before we began measurements of the perturbative Wilson loops. To increase statistics, we also created new ''parallel'' Langevin trajectories (keeping the same parameter ε) starting from a configuration already in equilibrium (given in replicas representing all orders in g) after changing the seeds for the white noise. Only in these cases the strategy of averaging over independent realizations of noise has been followed. Otherwise, subsequent sequences of noise are considered as independent.

We have observed that the autocorrelations increase on one side with increasing loop order and on the other side with increasing Wilson loop size. The perturbative Wilson loops have been measured after each 20th Langevin step to reduce autocorrelations. The integrated autocorrelation times are included in the error estimate of the measured quantities. Typically for the 1×1 Wilson loop the estimated autocorrelation was $O(1)$ at the lowest loop orders and increased up to $O(10)$ at the highest loop orders. So the relative errors significantly increase with the loop order. As a result, we have collected the following statistics in measuring the perturbative Wilson loops for the different chosen finite Langevin steps sizes and lattice volumes as shown in Table I. The statistics have to be understood as follows: The thermalization is not included, e.g., 21000 measurements at lattice volume L^4 with $L = 8$ and $\varepsilon = 0.01$ in the table corresponds to 420 000 Langevin steps in equilibrium. Those measurements are performed for all orders in g; the reached results are shown in the figures below.

Let us first discuss the accuracy and some problems we have met in performing the extrapolation to vanishing Langevin step size ε. Having several different expansion coefficients $W^{(n)}_{NM}(\varepsilon)$ for various ε values at a given loop order n available, we perform the extrapolation to the coefficient $W^{(n)}_{NM}$ corresponding to zero step size by a linear plus quadratic fit ansatz

$$W^{(n)}_{NM}(\varepsilon) = W^{(n)}_{NM} + A^{(n)}_{NM}\varepsilon + B^{(n)}_{NM}\varepsilon^2. \tag{17}$$

The ε behavior depends on the loop order n and the Wilson loop size $N \times M$, as well as on the lattice volume. To illustrate the overall behavior we present here results for the plaquette W_{11} and the Wilson loop W_{33} for lattice size $L = 12$.

The measured perturbative plaquette values $W^{(n)}_{11}$ at all integer loop orders $n > 0$ (remember that $W^{(0)}_{NM} \equiv 1$) behave in a similar way: they are all negative and tend to values different from zero which can be determined with very good accuracy. Except for $n = 2$ zero Langevin step size limit is approached from below with decreasing step size ε. The clearly nonvanishing fit results decrease monotonically in magnitude with increasing loop order. This is demonstrated in the left of Fig. 1; see also the tables in the Appendix. The coefficients of odd powers of g should be zero, because the action is unchanged under $g \leftrightarrow -g$. These nonloop coefficients are shown in the right-hand panel of Fig. 1. We observe that these coefficients are indeed orders of magnitude smaller than the coefficients for even powers of g. To show the quality of the $\varepsilon \to 0$ extrapolation we zoom into the small and large loop number behaviors of the expansion coefficients. This is demonstrated in Fig. 2. For better visibility, part of the expansion coefficients at low loop numbers n are multiplied by factors given in the figure.

Now we consider the Wilson loop W_{33}. In Fig. 3 we show how the loop and nonloop expansion coefficients for various Langevin step sizes behave as function of n. We observe that the noise of the nonloop coefficients is much larger than in the plaquette case, which has to be expected for Wilson loops with larger areas. For the smallest half-integer n the magnitude of the noise is larger than the actual (integer) loop results at much larger n. But still our criterion is fulfilled that a Wilson loop coefficient at a given loop order n should be larger than the magnitude of the noise for the adjacent $n - 1/2$ and $n + 1/2$ nonloop contributions.

TABLE I. Number of Wilson loops measurements up to loop order 20 at various lattice volumes L^4 and Langevin time steps ε.

ε	$L = 4$	$L = 6$	$L = 8$	$L = 12$
0.010	19522	16390	21000	5672
0.015	12182	13366	18500	⋯
0.020	11186	12726	18750	5464
0.030	10120	10210	17500	5334
0.040	9620	9466	17500	5200
0.050	9500	8500	16500	⋯
0.070	9500	8500	16250	5476

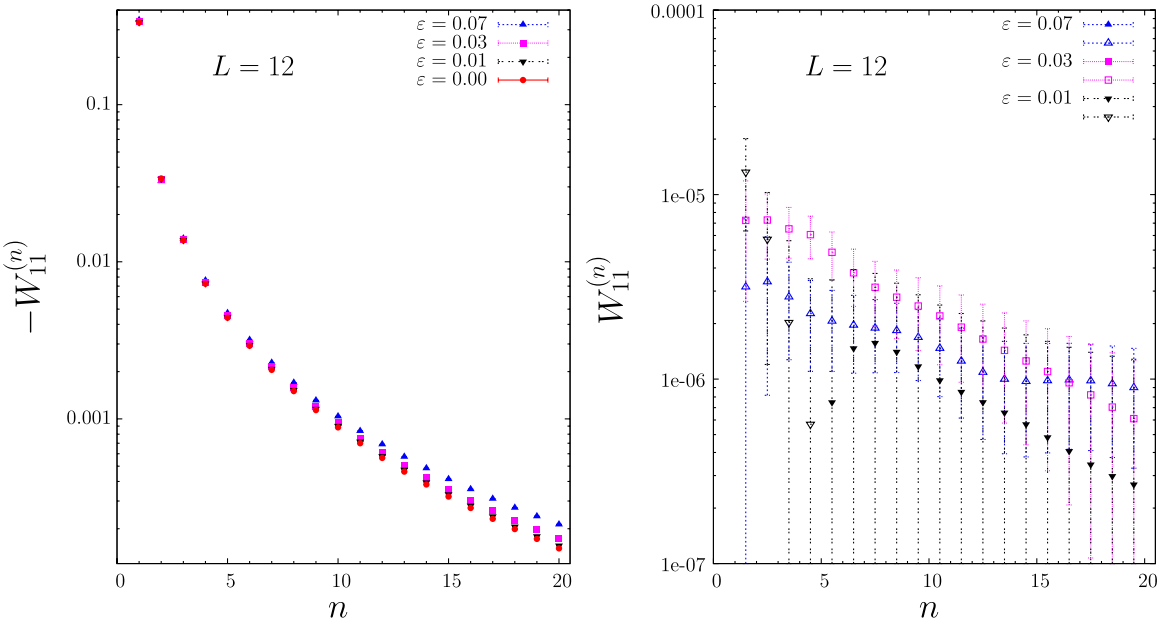

FIG. 1 (color online). Plaquette expansion coefficients $W_{11}^{(n)}$ at some finite ε at $L = 12$ versus loop number n. On the left-hand panel the loop expansion coefficients for integer n (signal) are shown together with their extrapolations $\varepsilon \to 0$. The right-hand panel shows the nonloop coefficients for half-integer n which are purely noise, and 2 or 3 orders of magnitude smaller than the integer coefficients. The open/full symbols denote positive/negative numbers.

Contrary to the plaquette case, the loop expansion coefficients alternate in sign for $n \leq 3$. In absolute value the step-size extrapolation $\varepsilon \to 0$ approaches the extrapolated value from above. For loop number $n = 4$ the situation is different (see the left panel of Fig. 4): The extrapolation of the expansion coefficient to zero Langevin step starts at a positive value $W_{33}^{(4)}(\varepsilon = 0.07)$, crosses "zero" with decreasing ε and points towards a negative value $W_{33}^{(4)}$ at zero Langevin step. Remember that near zero we have the "noise," shown in that figure as well, by the adjacent nonloop contributions 3.5 and 4.5. The magnitude of that

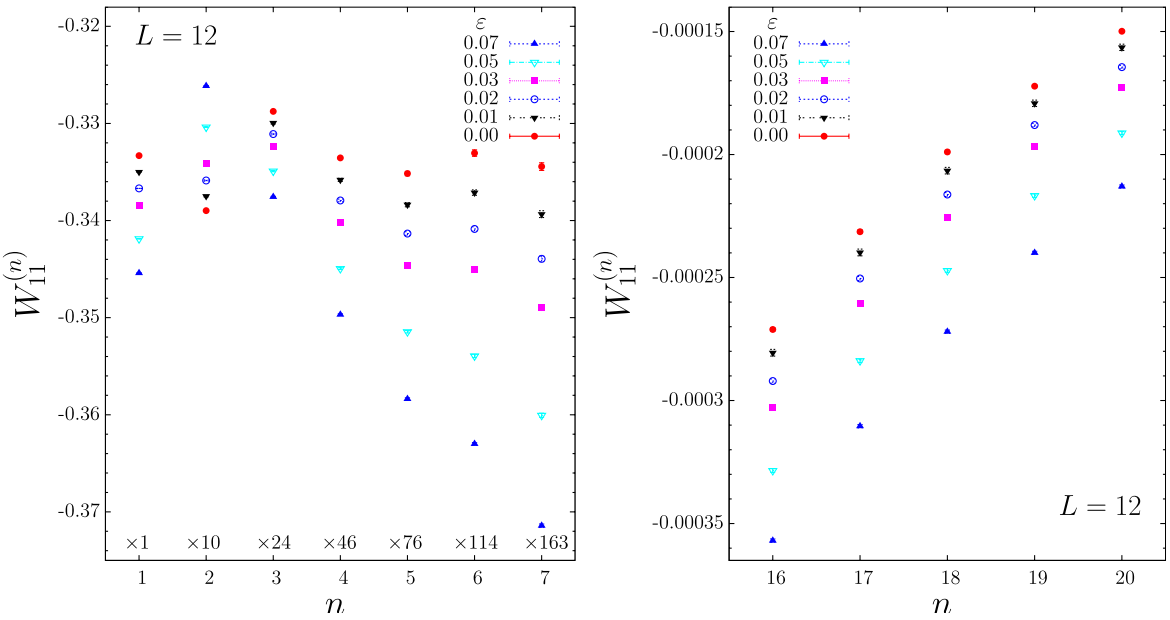

FIG. 2 (color online). Zoom in plot of left panel in Fig. 1 into small (left panel) and large (right panel) loop number region n for all finite ε. The full circles in red are the extrapolated $\varepsilon \to 0$ values. The coefficients in the left panel at different orders n are multiplied by factors to make them comparable in size to those at $n = 1$.

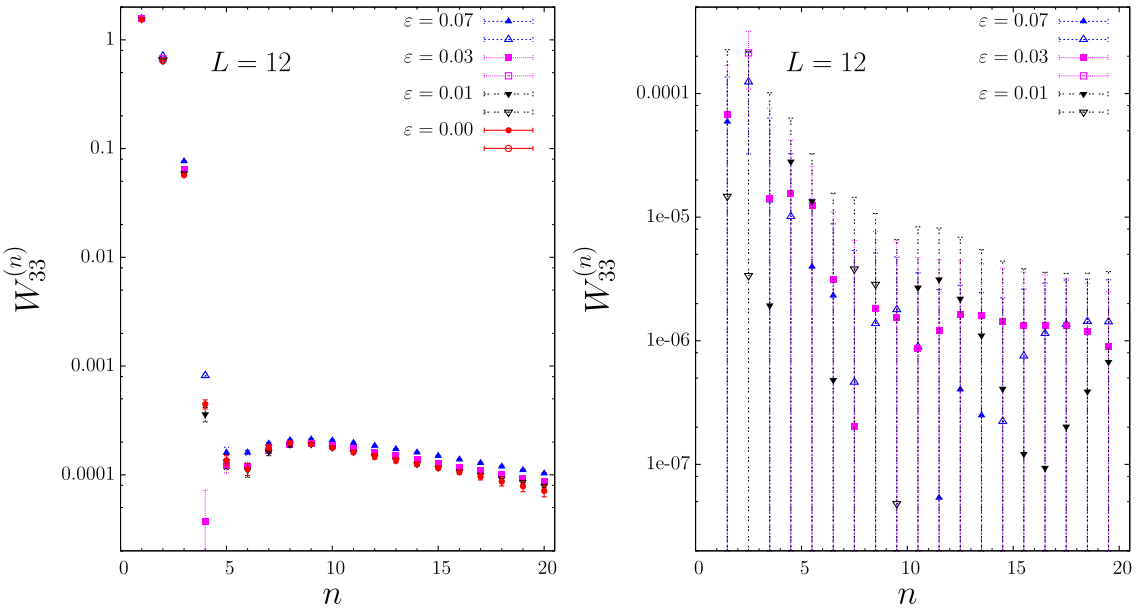

FIG. 3 (color online). Same as in Fig. 1 but for the Wilson loop expansion coefficients $W_{33}^{(n)}$.

noise is comparable to $W_{33}^{(4)}$ for $\varepsilon = 0.03$ only, and a reliable almost linear extrapolation to zero Langevin step is possible. For the next higher loop numbers $n > 4$ the extrapolation to zero Langevin step becomes clearly nonlinear as shown in more detail in the right panel of Fig. 4 for some loop numbers n. The extrapolated zero step size results are still clearly distinguishable from the adjacent nonloop expansion coefficients. Therefore, according to our criterion, those extrapolations can be considered as reliable. For larger loop numbers $n \geq 10$ the ε dependence becomes less nonlinear again. For those n the expansion coefficients of W_{33} as a function of n behave similar to those of the plaquette though their slope slightly differs.

In Fig. 5 we show some results for the loop coefficients (extrapolated to $\varepsilon = 0$) of elongated ($W_{N1}^{(n)}$, left panel) and square ($W_{NN}^{(n)}$, right panel) Wilson loops for various size N as a function of loop order n for a 12^4 lattice and compare them to the noise. At larger n, a behavior without sign

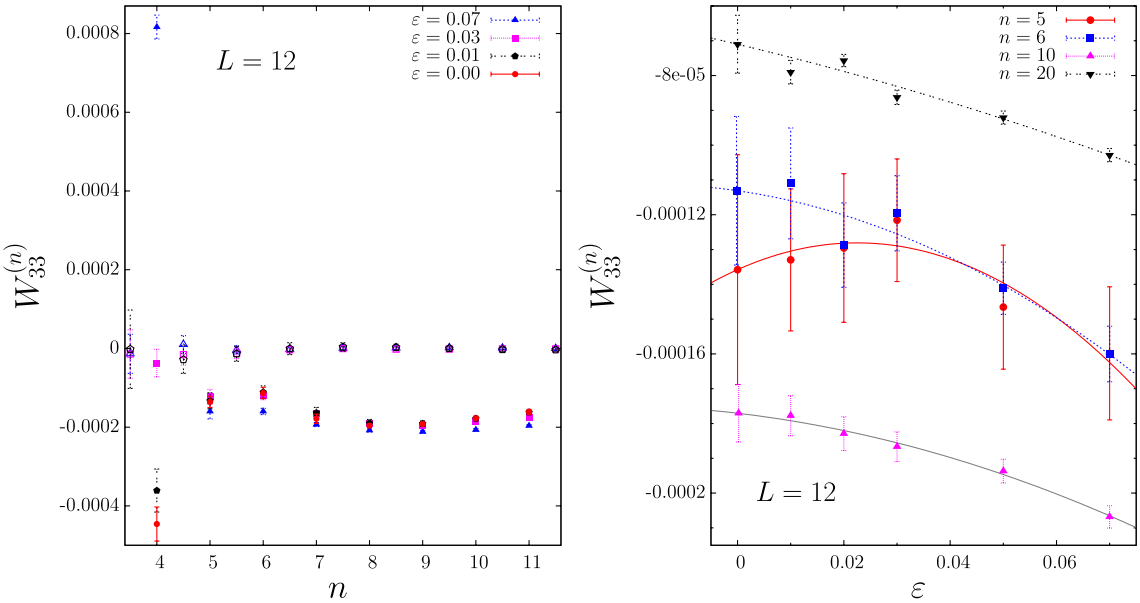

FIG. 4 (color online). The extrapolation to zero Langevin step for Wilson loop expansion coefficients $W_{33}^{(n)}$. Left panel: Zoom in of both panels in Fig. 3 in the region [3.5, 11.5]. Right panel: Detailed extrapolation to $\varepsilon \to 0$ for selected loop numbers.

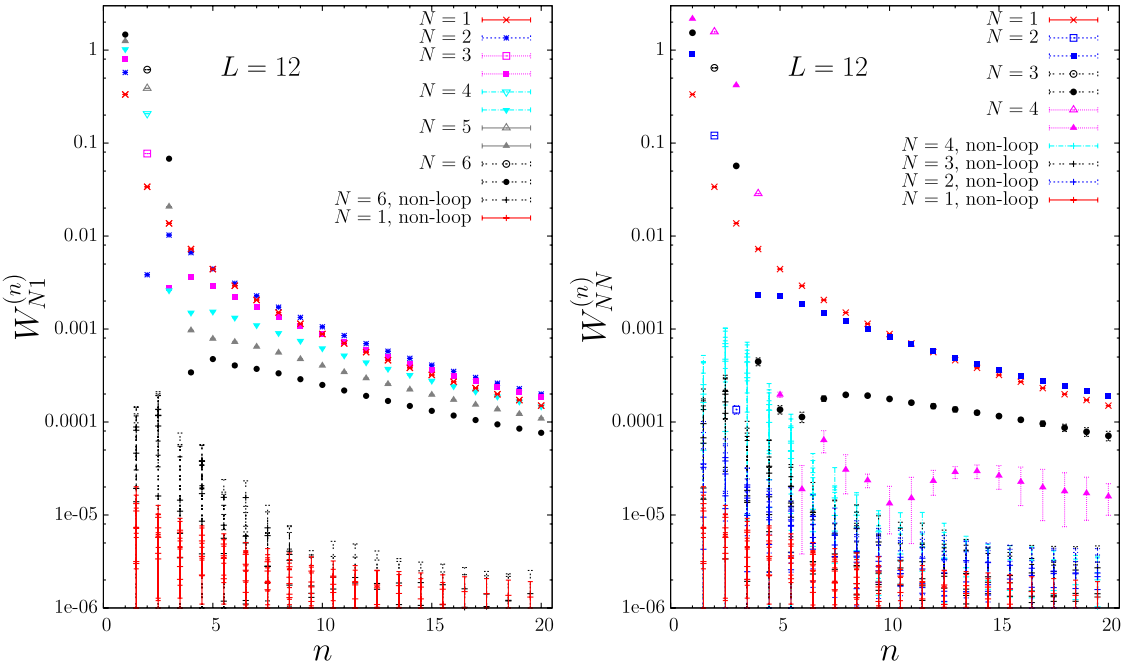

FIG. 5 (color online). Selected loop coefficients $W_{NM}^{(n)}$ for $L = 12$ versus loop order n together with typical values in magnitude of nonloop coefficients. Positive/negative signs of the coefficients are given by open/full symbols, all $W_{11}^{(n)} < 0$, $W_{21}^{(n)} < 0$. Left panel: elongated Wilson loops $N \times 1$ with $N = 1, \ldots, 6$. Right panel: square Wilson loops $N \times N$ with $N = 1, \ldots, 4$.

changes is observed for all considered Wilson loops that could be interpreted as "asymptotic". We note that the precision of the extrapolated loop coefficients for the larger Wilson loops drops down and also the signal to noise ratio decreases. Still, the signal for the shown Wilson loops is clearly above the noise for all orders. For square Wilson loops with $N \geq 4$ (not shown) or other larger Wilson loops the statistics were insufficient to get a clear signal out of the noise for larger orders (see also the Appendix). In the analysis below we concentrate on the smallest Wilson loops.

In addition we have to raise the question about the infinite volume limit of the series. In the perturbative series the leading finite-size correction is expected to be proportional to $1/L^4$. For additional nonleading corrections we tried the heuristic ansatz

$$W_{NM,L}^{(n)} = W_{NM,\infty}^{(n)} + a_{NM}^{(n)} \frac{1}{L^4} + b_{NM}^{(n)} \frac{\log L}{L^6}, \qquad (18)$$

which describes well the L-dependence of one-loop and two-loop coefficients of the perturbative Wilson loops for various loop sizes. Those coefficients are known from standard finite volume lattice perturbation theory [16] (the basic formulas have been given in Ref. [17]). Note that the one-loop and two-loop NSPT coefficients reproduce the finite volume lattice perturbation theory reasonably well as shown in Table II for some examples.

For lower loop orders a simple $1/L^4$ dependence was sufficient in the fits in agreement with Ref. [17]. Higher loop coefficients, however, need further corrections which we have chosen in the form (18). In Fig. 6 we show two selected extrapolations for the one-loop and ten-loop ex-

TABLE II. Comparison of one-loop and two-loop results for NSPT and the finite volume standard lattice perturbation theory [16].

W_{NN}	L	NSPT (1-loop)	Bali (1-loop)	NSPT (2-loop)	Bali (2-loop)
W_{22}	4	−0.87468(13)	−0.87500	0.10404(07)	0.10406
	6	−0.90752(12)	−0.90762	0.11830(10)	0.11837
	8	−0.91147(03)	−0.91141	0.11998(02)	0.11993
	12	−0.91264(02)	−0.91261	0.12043(01)	0.12038
W_{33}	6	−1.50088(30)	−1.50093	0.60906(34)	0.60866
	8	−1.52849(12)	−1.52803	0.63654(08)	0.63632
	12	−1.53552(06)	−1.53533	0.64388(01)	0.64360
W_{44}	8	−2.14092(23)	−2.14016	1.52436(28)	1.52331
	12	−2.17001(10)	−2.16922	1.57160(10)	1.57006

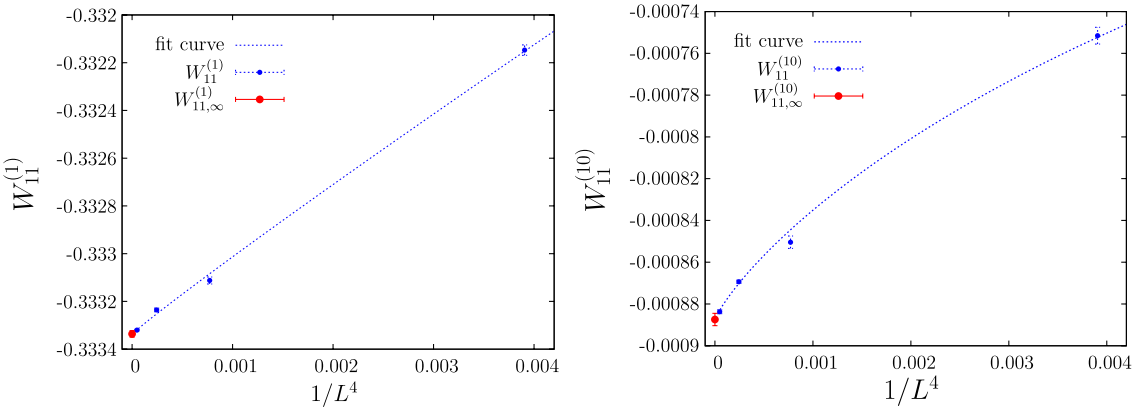

FIG. 6 (color online). Extrapolation $L \to \infty$ for $W_{11}^{(n)}$ for loop orders $n = 1$ (left panel) and $n = 10$ (right panel).

pansion coefficient. From the volume dependence of all orders and sizes of the Wilson loop we conclude that we can treat the lattice volume 12^4 as being already near to the infinite volume limit. Therefore, in the subsequent analysis we use that lattice size as a reasonable approximation for volume independent results of the series. In the Appendix we present the expansion coefficients for all available lattice volumes and Wilson loop sizes.

III. PERTURBATIVE SERIES OF WILSON LOOPS AT LARGE ORDERS

There is plenty evidence that perturbative series in continuum QCD are divergent, at best asymptotic. This would mean that, beginning from some perturbative order $n > n^\star$, the coefficients of the series should grow factorially. The situation might be different for perturbative series on finite lattices. Here we have both ultraviolet and infrared cutoffs and the growth could be modified significantly. With our computed coefficients of the loop expansion up to order $n = 20$ we are able to check this to a so far inaccessible level.

For finite lattices one could try to use the raw NSPT coefficients for evaluating the corresponding underlying infinite series. This requires one to deduce a kind of asymptotic model providing the complete perturbative answer. Formally, one can use such a model designed for finite lattices also in a version adapted to the coefficients extrapolated to $L \to \infty$. Although the extrapolation seems to yield smooth limits, it is certainly not allowed to sum a series based on these extrapolated coefficients up to infinity. In this case there exist at least two possibilities. The first consists of taking into account possible renormalon effects and estimating the truncated tail of the series (cf., e.g., [9]). This procedure, however, strongly depends on whether a clear factorial growth of the coefficients in the perturbative region under consideration has been identified. We will see that this is very difficult to justify from our results. A second possibility consists in applying boosting, i.e., a rearrangement of the series resulting in a (rather) stable plateau of the truncated sum as a function of the maximal perturbative order n^* that is included, and to use this as the final perturbative result at a given coupling.

A. Plaquette

In 2001, when only the first 10 loops of the plaquette series as expansion in the bare coupling were known from Ref. [7], some of the present authors tried plotting the data in various ways in order to find a fit ansatz which could describe the known data and would be able to predict the unknown higher coefficients [18]. A logarithmic plot of $W_{11}^{(n)}$ against n shows a curve with decreasing slope, well described by an asymptotic behavior,

$$W_{11}^{(n)} \sim n^{-(1+\gamma)} u^n, \tag{19}$$

i.e., an exponential in n multiplied by a power of n (see Fig. 1 and the tables in the Appendix). This is a somewhat unexpected result, because a series of this type has a finite radius of convergence, $g^2 < 1/u$, and sums to give a result with a power-law singularity of the form

$$(1 - ug^2)^\gamma. \tag{20}$$

A more sensitive way of showing the large n behavior of a series is the Domb-Sykes plot [19]. If the series has the form

$$\sum_n c_n g^{2n}, \tag{21}$$

we calculate r_n, the ratio of neighboring coefficients,

$$r_n \equiv \frac{c_n}{c_{n-1}}, \tag{22}$$

and plot it as a function of $1/n$. The intercept as $1/n \to 0$ (if the limit exists) gives the radius of convergence. The behavior for small $1/n$ (i.e., large n) tells us the nature of the dominant singularity. A function with the power-law singularity (20) has the expansion

$$(1-ug^2)^\gamma = 1 - \gamma u g^2 + \cdots + \frac{\Gamma(n-\gamma)}{\Gamma(n+1)\Gamma(-\gamma)}(ug^2)^n + \cdots, \tag{23}$$

which leads to the ratio of neighboring coefficients depending on the parameters u and γ,

$$\frac{c_n}{c_{n-1}} = u\left(1 - \frac{1+\gamma}{n}\right). \tag{24}$$

Therefore, the Domb-Dykes plot c_n versus $1/n$ is a straight-line graph.

The actual Domb-Sykes plot for the measured perturbative plaquette showed a small curvature. To allow for this we added one more parameter and made a fit of the form

$$r_n = u\left(1 - \frac{1+\gamma}{n+s}\right). \tag{25}$$

This described the data for $n \in [3, 10]$ well, with the parameter values [18],

$$u = 0.961(9), \qquad \gamma = 0.99(7), \qquad s = 0.44(10). \tag{26}$$

We now have 10 more coefficients. How well do the fit parameters (26) predict the new data? In Fig. 7 we compare the current data with the prediction made in 2001.

The data lie very near the prediction. We have doubled the maximum n value without seeing any breakdown of the behavior seen at lower n. In particular, the series still looks like a series with a finite range of convergence, $g^2 < 1.04$.

B. A model for summing up the Wilson loop series

Now we have in addition also Wilson loops larger than the plaquette at our disposal. In Fig. 8 we show the coefficient ratios r_n for some small size Wilson loops for $n \geq 5$. We have seen that at large order n the coefficients in the plaquette series have the asymptotic behavior of (19). What is the asymptotic behavior of the other Wilson loops? Is it similar?

A sensitive way to investigate this is to look at the ratio between the coefficients of the Wilson loops series and the plaquette series. If both have similar behaviors at large order n,

$$\frac{W^{(n)}_{NM}}{W^{(n)}_{11}} \sim \frac{n^{-(1+\gamma')}(u')^n}{n^{-(1+\gamma)}u^n} = n^{(\gamma-\gamma')}\left(\frac{u'}{u}\right)^n. \tag{27}$$

We plot the ratio (27) for various NM values in Fig. 9 as a log-log plot against n. The plot shows that at large n the ratio scales like a power of n, suggesting that the parameter u in (19) is the same for all Wilson loops, but the power γ depends on the size of the loop. Therefore, $u' = u$ to a very good approximation. This means that for all Wilson loops the series have the same apparent radius of convergence, $g^2 < 1/u$. However the curves for different Wilson loops have different slopes at large n, indicating different asymptotic powers of n, i.e., different values of γ.

In Fig. 8 one clearly recognizes that for larger loop sizes the ratios deviate from the almost perfect straight line behavior seen for W_{11}. This deviation can be described rather well by a modification of (25) taking into account some curvature, especially for larger loop sizes $N \times M$. Parametrizing these effects by an additional parameter p we make the ansatz

$$r_n = \frac{c_n}{c_{n-1}} = u\left(1 - \frac{1+\gamma}{n}\right) + \frac{p}{n(n+s)}, \tag{28}$$

where the first term is the asymptotic form (24) without curvature. Relation (28) can be transformed into a recursion relation,

$$c_n = \begin{cases} r_n c_{n-1}, & \text{if } n > n_0, \\ c_{n_0}, & \text{if } n = n_0. \end{cases} \tag{29}$$

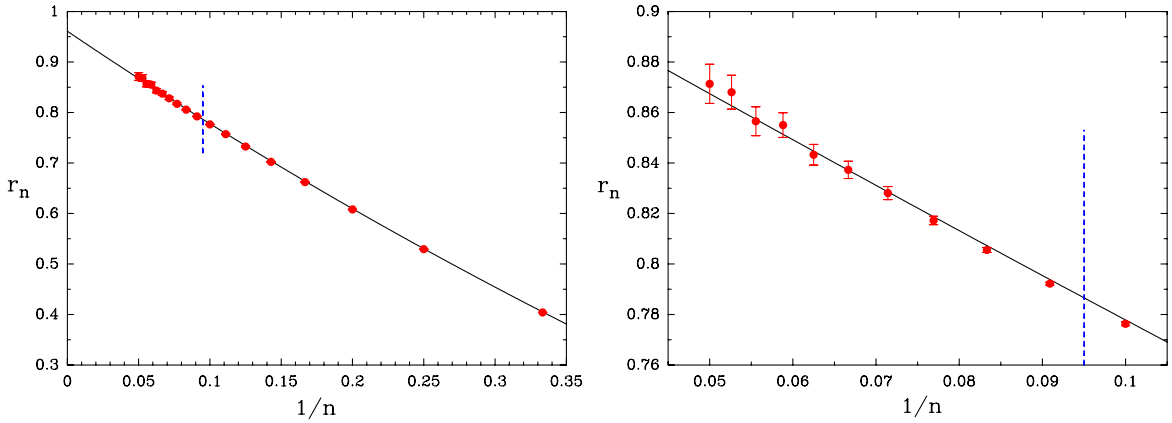

FIG. 7 (color online). Current ratio data for the plaquette, compared with the prediction of 2001 [18], plotted with the original parameters. The prediction was based on data with $n \leq 10$, i.e., to the right of the vertical blue bar. The second figure zooms in on the region of new data.

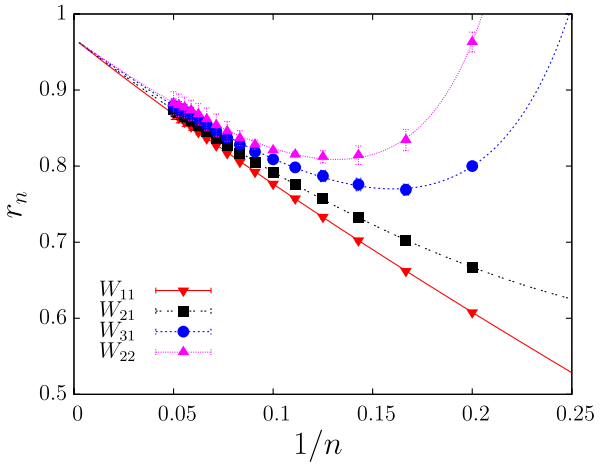

FIG. 8 (color online). Domb-Sykes plots for W_{NM} for $n \geq 5$ together with the fit result using (28).

Here c_{n_0} is the input value for some lowest measured perturbative coefficient $W_{NM}^{(n_0)}$ at loop order $n = n_0$ to begin the recursive reconstruction. Relation (29) can be solved to

$$c_{n,\mathrm{hyp}} = d_{n_0} \frac{(\sigma-\tau-1)_n(\sigma+\tau-1)_n}{(s+1)_n n!} u^n,$$
$$\tau = \frac{1}{2}\sqrt{(\gamma+s+1)^2 - 4p/u}, \tag{30}$$
$$\sigma = \frac{s+3-\gamma}{2},$$

with $(a)_n \equiv \Gamma(a+n)/\Gamma(a)$ being the Pochhammer symbol. The coefficient d_{n_0} is given by

$$d_{n_0} = \frac{n_0! c_{n_0}}{u^{n_0}} \frac{\prod_{i=1}^{n_0}(s+i)}{\prod_{k=1}^{n_0}((\sigma-2+k)^2-\tau^2)}. \tag{31}$$

Accepting such a parametrization one can follow different strategies:

(i) Use the raw coefficients c_n and/or $c_{n,\mathrm{hyp}}$ fixed by the fitted values of the parameters in the loop order range $1 \leq n \leq 20$ as determined by the NSPT computation to investigate the perturbative series. This will be done in Sec. III C.

(ii) Assume that the coefficients $c_{n,\mathrm{hyp}}$, found as solution of (29), belong to an infinite series and try to sum up the series on a finite lattice. This will be discussed in the following text.

The infinite series we want to compute is defined by

$$W_{NM,\infty}^{(n_0)} = 1 + \sum_{n=1}^{n_0} c_n g^{2n} + \sum_{n=n_0+1}^{\infty} c_{n,\mathrm{hyp}} g^{2n}$$
$$\equiv 1 + \sum_{n=1}^{\infty} W_{NM,\mathrm{hyp}}^{(n)} g^{2n}, \tag{32}$$

where the first n_0 coefficients $c_n \equiv W_{NM}^{(n)}$ are given by the NSPT measurements and the $c_{n,\mathrm{hyp}}$ are the solutions of (29). For later use we have introduced the general coefficients $W_{NM,\mathrm{hyp}}^{(n)}$. The matching condition for (32) is that at n_0 we have $c_{n_0} = c_{n_0,\mathrm{hyp}}$. Introducing the hypergeometric function ${}_2F_1$,

$$2F_1(a,b;c;t) = \sum_{n=0}^{\infty} A_n t^n \equiv \sum_{n=0}^{\infty} \frac{(a)_n (b)_n}{(c)_n n!} t^n, \tag{33}$$

we get the closed expression

$$W_{NM,\infty}^{(n_0)} = 1 + \sum_{n=1}^{n_0} (c_n - d_{n_0} A_n u^n) g^{2n}$$
$$+ d_{n_0}[{}_2F_1(\sigma-\tau-1, \sigma+\tau-1; s+1; ug^2) - 1]. \tag{34}$$

The result expressed in terms of ${}_2F_1(a,b;c;ug^2)$ has a branch cut discontinuity at the positive g^2-axis for $g^2 > 1/u$. This means that the parameter u in (28) [just as well as in (25)] determines the convergence radius: for $g^2 < 1/u$ the series can be summed up to $n = \infty$ without analytic continuation into the complex plane. All parameters u, γ, p, s depend on the corresponding underlying data set. As discussed above (see also Fig. 9) we will assume that the convergence radius is the same for all Wilson loop sizes which implies a common value for u.

We found that Wilson loops larger in size than the plaquette (e.g., W_{21}, W_{31}, W_{22}) give rise to ratios r_n (for $n < 5$) that show a pronounced oscillating behavior. Therefore, we restrict the fit of the ratio function (28) to the data for $n > n_0 = 4$ only. The fit results are shown in Fig. 8 as thin lines.

It should be pointed out that fitting the parameters (u, γ, p, s) in ansatz (28) to the NSPT data is nontrivial. We have determined the optimal values by minimizing the function

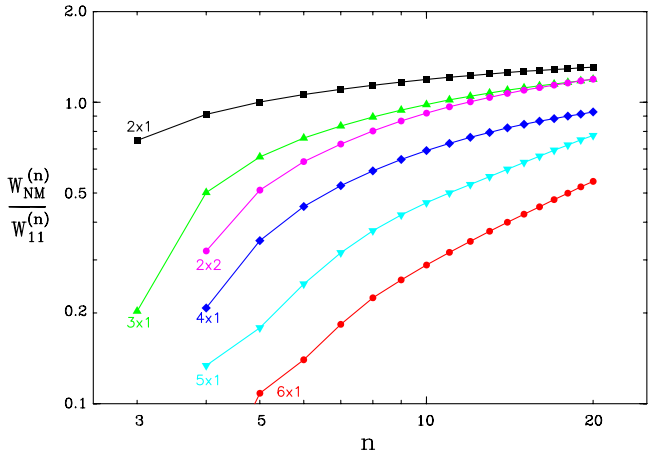

FIG. 9 (color online). A log-log plot of the ratio (27), plotted for different sizes of Wilson loops. To guide the eyes, the data points for the loop orders are connected by lines.

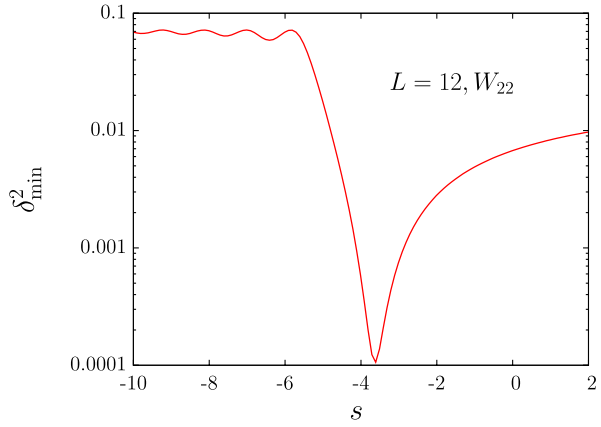

FIG. 10 (color online). $\delta^2_{\rm min}$ as function of parameter s for W_{22}.

$$\delta^2(u,\gamma,p,s) = \sum_{n=n_0+1}^{20} \frac{[r_n(u,\gamma,p,s) - r_n(\mathrm{NSPT})]^2}{[r_n(\mathrm{NSPT})]^2}, \tag{35}$$

where r_n(NSPT) are the ratios computed from the corresponding NSPT data. The most sensitive parameter in (28) is s. Therefore, we vary s over a certain range $s_{\rm min} < s < s_{\rm max}$ by a small increment Δ_s as $s_0(k) = s_{\rm min} + k\Delta_s$ (k-integer) and minimize $\delta^2(u,\gamma,p,s_0(k))$ with respect to (u,γ,p) at every $s_0(k)$ which is held fixed. The smallest of all minimized $\delta^2_{\rm min}(u,\gamma,p,s_0(k))$ defines the starting set $(u_\star,\gamma_\star,p_\star,s_0(k_\star))$ for a final minimization fit—now with respect to all parameters (u,γ,p,s). In Fig. 10 we show one example for $\delta^2_{\rm min}$ for W_{22} with $n_0 = 4$. One recognizes a couple of shallow local minima (besides the absolute one) where minimization procedures could have been trapped. In Table III we give the results of our minimal fit function and the final fit parameters for various Wilson loops. The given errors $(\Delta u, \Delta\gamma, \Delta p, \Delta s)$ are the extreme values within the error ellipsoid obtained from the relation

$$\begin{aligned}&\delta^2(u^\star + \Delta u, \gamma^\star + \Delta\gamma, p^\star + \Delta p, s^\star + \Delta s)\\ &\quad = 2\delta^2(u^\star,\gamma^\star,p^\star,s^\star),\end{aligned} \tag{36}$$

where $(u^\star,\gamma^\star,p^\star,s^\star)$ are the best fit parameters. For extrapolation of the perturbative series we use hypergeometric fits in the interval [5, 20]. Fits to the coefficients in this range are excellent, with relative errors $\leq 0.5\%$.

TABLE III. Minimal value of $\delta^2_{\rm min}$ and resulting fit parameters. The fit range in n is [5,20].

W_{NM}	$\delta^2_{\rm min}$	u	γ	p	s
W_{11}	8×10^{-6}	0.9694(4)	1.13(5)	$1.5^{+1.3}_{-0.6}$	$0.7^{+3.0}_{-1.8}$
W_{21}	1×10^{-5}	0.9694(5)	1.02(4)	1.6(5)	−1.4(8)
W_{31}	2×10^{-5}	0.9694(6)	0.91(4)	1.7(2)	−3.3(2)
W_{22}	4×10^{-5}	0.9694(9)	0.82(4)	1.9(2)	−3.9(1)

The hypergeometric fit still gives a fairly good description of the data all the way down to $n = 1$. For most loop sizes a fit from $n = 1$ to 20 describes the data within ~5%, except for the 2×1 loop, which has some errors, $\approx 10\%$. Given that the coefficients vary through 4 orders of magnitude in this interval, an error of 5% or 10% is still impressive.

All the Wilson loops show rather similar behavior at large order n; see Fig. 11. At small n they look quite different from the plaquette, with a mixture of positive and negative terms. It is interesting that there is often a "notch" just before the asymptotic region begins, i.e., a particularly steep drop to a small coefficient, followed by a jump back up again. This is particularly dramatic in the 2×2 Wilson loop, where the $n = 3$ coefficient is about 600 times smaller than the $n = 2$ coefficient. The notch gives rise to big changes in r_n, for example for the 2×2 loop we have

$$\begin{aligned}\ldots, r_2 &= -0.1319, \qquad r_3 = +0.0016,\\ r_4 &= -11.98, \qquad r_5 = +0.9722, \ldots.\end{aligned} \tag{37}$$

The notch corresponds to the singularity in the Domb-Sykes plot. The anomalously large r_n value occurs when n is close to the pole at $n = -s$ in (28). This is demonstrated in Fig. 12 where the fit to the parameters has been extended to the range $n \in [2, 20]$. Using this fit range one clearly recognizes the corresponding pole terms.

Our analysis shows that we can reproduce our NSPT data up to order $n = 20$ for Wilson loops of moderate size (at least the elongated ones) with this hypergeometric model sufficiently well. This means that we do not find any evidence for a factorial behavior which should result in a behavior $r_n \sim n$. In Sec. II B we showed that in the range $4 \leq L \leq 12$ the volume dependence of each individual perturbative coefficient is rather smooth and already very weak at sizes like $L \approx 12$. So we do not expect a significant change extrapolating the results to infinite lattice size.

Even beyond the apparent radius of convergence ($g^2_c = 1/u$, $\beta_c \approx 5.82$) the perturbative series still has some information on the Wilson loops. In that case the terms in the series decrease initially, before reaching a minimum and then growing. Summing the series up to the minimum term would give an approximation to the Wilson loop. The minimum term in the series can be estimated from the condition on the ratio of neighboring coefficients in (22) $r_{n_{\rm min}} g^2 = 1$. The corresponding minimal number $n_{\rm min}$ in the summation is approximately (neglecting the parameters s and p)

$$n_{\rm min} \approx \frac{(1+\gamma)ug^2}{ug^2 - 1} = \frac{6u(1+\gamma)}{6u - \beta} \approx \frac{12}{\beta_c - \beta}, \tag{38}$$

for $\beta < 6u$. So, at $\beta = 5.7$ we would have to sum about 100 terms before reaching the minimum (assuming, of course, that the hypergeometric form remains applicable), and even at $\beta = 5.2$ ($g^2 = 1.15$) we would still have about

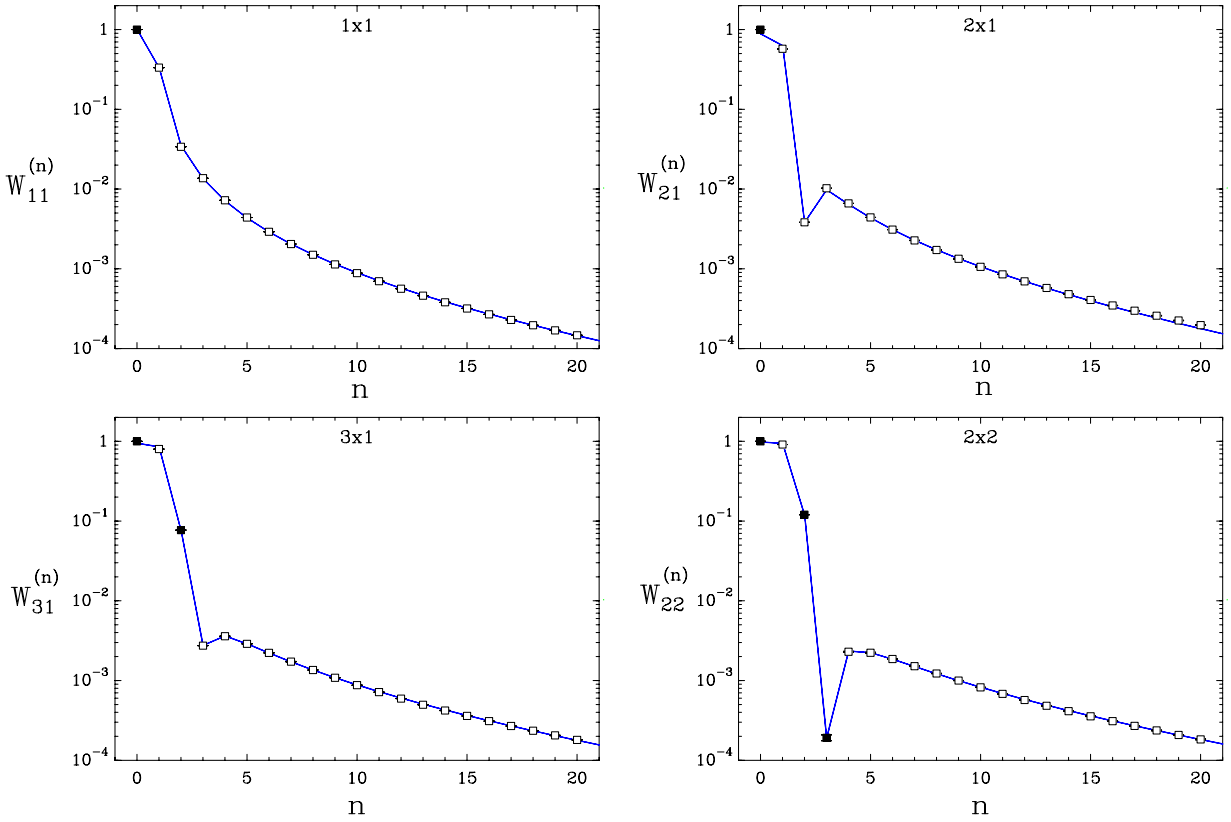

FIG. 11 (color online). The hypergeometric fit to the coefficients $W_{NM}^{(n)}$ for the four small Wilson loops. Solid symbols represent positive terms, open symbols are negative terms. The blue line is an equal weight fit, including all points from $W_{NM}^{(0)}$ to $W_{NM}^{(20)}$. The agreement is remarkably good.

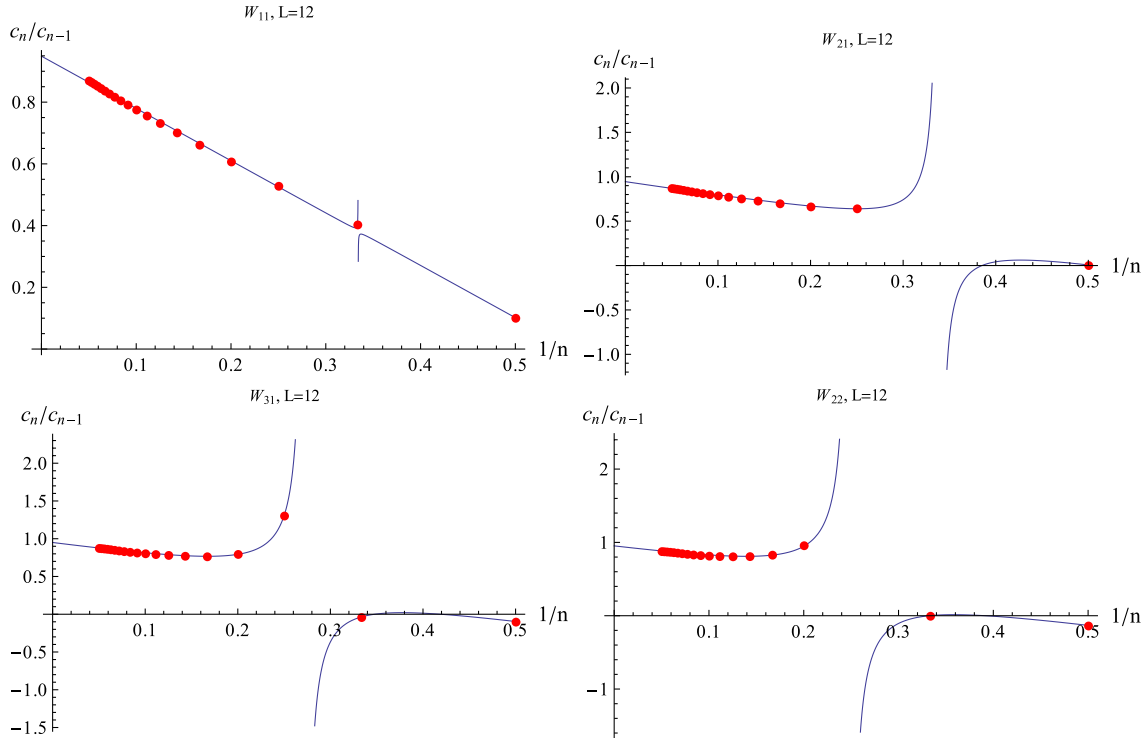

FIG. 12 (color online). Domb-Sykes plots for W_{NM} with fits to the parameters in the range $n \in [2, 20]$.

20 decreasing terms before reaching the minimum term. To stay on the safe side, we have not used any data beyond the apparent convergence radius g_c in our analysis of nonperturbative Wilson loops described below. We have restricted ourselves to $\beta \geq 5.85$, i.e., $g^2 \leq 1.026$.

C. Boosted perturbation theory

It is well-known that the bare lattice coupling g is a bad expansion parameter by virtue of lattice artifacts like tadpoles. There is hope that, by redefining the bare coupling g into a boosted coupling g_b and the corresponding rearrangement of the series, a better convergence behavior can be achieved [20]. For the case of perturbative Wilson loops this idea has been applied for the first time by Rakow [8].

Let us denote the perturbative Wilson loop summed up to order $n^\star$ using the bare coupling g by

$$W_{NM}(g, n^\star) = 1 + \sum_{n=1}^{n^\star} W_{NM}^{(n)} g^{2n}, \tag{39}$$

and call in the following any series in g^2 a "naive series." We define the boosted coupling as

$$g_b^2 = \frac{g^2}{W_{11}(g, n^\star)}. \tag{40}$$

The corresponding "boosted series" for an arbitrary Wilson loop W_{NM} is then given by

$$W_{NM,b}(g_b, n^\star) = 1 + \sum_{n=1}^{n^\star} W_{NM,b}^{(n)} g_b^{2n}, \tag{41}$$

with coefficients $W_{NM,b}^{(n)}$ to be calculated from $W_{NM}^{(k)}$ and $W_{11}^{(l)}$ with $k, l \leq n$. Setting

$$W_{NM}(g, n^\star) = W_{NM,b}(g_b, n^\star), \tag{42}$$

and inserting (40) into the right- hand side of (42), we can compute the boosted coefficients $W_{NM,b}^{(n)}$ order by order.

It should be emphasized that the prescribed procedure is done by solving a hierarchical set of recursive equations. Especially for large loop orders n these equations involve hundreds or thousands of terms. Using the NSPT raw data $W_{NM}^{(n)}$ with their errors gives rise to significant numerical instabilities in the boosted result for larger n. Therefore, it turned out to be advantageous to use the coefficients $W_{NM,\mathrm{hyp}}^{(n)}$ (32) as input for the recursive equations. Using that form up to loop order $n \leq 20$ means that we are smoothing the data of the naive series. In addition we are in the position to extend the maximal loop order beyond $n = 20$. This leads to a stable numerical result for the boosted coefficients $W_{NM,b,\mathrm{hyp}}^{(n)}$. An additional improvement can be achieved by replacing the lowest order perturbative coefficients at $L = 12$ by the corresponding coefficients of the infinite volume limit. In the Appendix we give those numbers for the one-loop and two-loop coefficients obtained in the diagrammatic approach [21–23].

In Fig. 13 we compare the perturbative coefficients of the plaquette for the NSPT raw data $W_{11}^{(n)}$ with the $W_{11,b}^{(n)}$ calculated from the raw data and the $W_{11,b,\mathrm{hyp}}^{(n)}$. The boosted coefficients obtained via the model show a smooth decreasing behavior with much smaller errors than the boosted coefficients based on the raw data, all the way down to the highest order $n = 20$. The superior result concerning the error is due to the fact that the errors of the model-fitted coefficients are computed from the correlated errors of the parameters (u, γ, p, s) as discussed in the preceding section. The errors of the boosted coefficients (when constructed from the raw data) are calculated with standard error propagation through the set of recurrence equations involving thousands of terms. Since the perturbative plaquette (as the nonperturbative plaquette) is less than one, $W_{11}(g, n^\star) < 1$, it is clear from (40) that $g_b^2 > g^2$. On the other hand, we find $|W_{11,b}^{(n)}| \ll |W_{11}^{(n)}|$ for $n > 4$ as shown in Fig. 13. We remark that also the boosted coefficients are characterized by oscillating signs as function of the loop order n for smaller n (open versus filled symbols).

The above mentioned numerical problems relating the boosted series to the naive series obtained directly from NSPT would be less severe if we could start from a coupling constant which was closer to g_b. Therefore in Ref. [8] one of us proposed a simulation with a shifted "reference" coupling constant, g_{ref}. Instead of simulating NSPT with the action (3), we could use the slightly modified action

$$S_{\mathrm{ref}}[U] = 6\left(\frac{1}{g_{\mathrm{ref}}^2} + \hat{r}_1 + \hat{r}_2 g_{\mathrm{ref}}^2\right) \times \sum_P \left[1 - \frac{1}{6}\,\mathrm{Tr}(U_P + U_P^\dagger)\right], \tag{43}$$

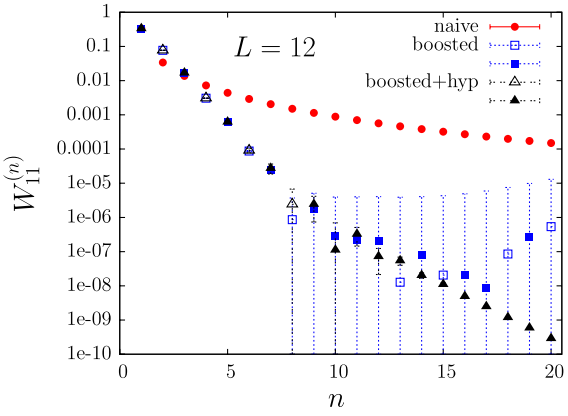

FIG. 13 (color online). Comparison of perturbative coefficients for the naive series ($W_{11}^{(n)}$), the boosted series from NSPT raw data ($W_{11,b}^{(n)}$) and the boosted series using the hypergeometric model ($W_{11,b,\mathrm{hyp}}^{(n)}$). The boosted coupling (40) is used; positive/negative signs of the coefficients are given by open/full symbols.

TABLE IV. Coefficients for the plaquette in boosted perturbation theory, calculated using the modified action (43) on a 12^4 lattice. They are compared to the corresponding coefficients from the NSPT raw data (second column) and the hypergeometric model data (third column). The loop order n given in the table is restricted by the order used in Ref. [8].

n	$W^{(n)}_{11,b}$ from (43)	$W^{(n)}_{11,b}$ from NSPT raw data	$W^{(n)}_{11,b}$ from (32)
1	−0.333334(42)	−1/3	−1/3
2	0.077187(30)	0.0772001181(8)	0.0772001181(8)
3	−0.016817(10)	−0.0168321(4)	−0.0168321(4)
4	0.0030488(10)	0.0030612(3)	0.0030612(3)
5	−0.0006101(14)	−0.00061867(9)	−0.000620(11)
6	0.0000831(7)	0.000087(2)	0.0000911(14)
7	−0.00002209(34)	−0.000024(2)	−0.0000275(89)
8	−0.00000007(30)	0.0000009(28)	0.0000024(43)
9	−0.00000138(11)	−0.0000017(33)	−0.0000024(17)
10	−0.00000042(8)	−0.00000029(360)	−0.00000011(58)
11	−0.000000201(12)	−0.00000022(380)	−0.00000033(18)
12	−0.000000087(14)	0.000000012(3877)	−0.000000073(51)

where now U_P is expanded as a power series in $g_{\rm ref}$ rather than g. Physically, the action is still the usual plaquette action—all we have done is to redefine the coupling constant. This modified action leads to changes in the drift term of (4). The advantage is that the simulation now gives us a series for the plaquette in terms of the coupling $g_{\rm ref}$, related to the bare coupling by

$$\frac{1}{g^2} = \frac{1}{g^2_{\rm ref}} + \hat{r}_1 + \hat{r}_2 g^2_{\rm ref}. \tag{44}$$

If we choose the parameters $\hat{r}_1$ and $\hat{r}_2$ well, the new intermediate coupling will be close to the boosted coupling, so the transformation from $g_{\rm ref} \to g_b$ will be numerically stable and will not introduce large uncertainties as in the transformation from $g^2 \to g^2_b$.

In Ref. [8] simulations have been performed with $\hat{r}_1 = 1/3$, $\hat{r}_2 = 0.033911$. These values were chosen such that $g^2_b = g^2_{\rm ref} + O(g^8_{\rm ref})$, making the transformation between the two couplings numerically robust. The resulting boosted series is shown in Table IV. The results are compatible with those found by transforming both the naive series from the NSPT raw data and from the hypergeometric model, respectively, but the error bars are now considerably reduced. In particular, the change in the behavior beyond $n = 8$, from an alternating series to a single-sign series is confirmed in this calculation. So far we have only applied this method to the series describing the plaquette, but we expect that it would also be useful for the larger Wilson loops.

The successful hypergeometric model fit to the NSPT raw data (as presented in the preceding section) and the very smooth behavior of the boosted coefficients based on the fit formula (34) allows us to extend the accessible loop order for the coefficients both in the naive and boosted series far beyond $n = 20$ loops. In Fig. 14 the corresponding coefficients for W_{11}, W_{21}, W_{31} and W_{22} are shown throughout the extended range of loop orders $n \leq 40$ relying on the information contained in the set of smoothed data represented by the hypergeometric model.

In Fig. 15 we compare the effect of truncating the sum at order $n^\star$ for the naive and boosted series, both on the basis of the hypergeometric model. The corresponding truncation error $T_{NM}(n^\star)$ is defined by

$$T_{NM}(n^\star) = \frac{|W_{NM}(n^\star) - W^{(n_0)}_{NM,\infty}|}{W^{(n_0)}_{NM,\infty}}, \tag{45}$$

where $W_{NM}(n^\star)$ is either the naive $[W_{NM}(g, n^\star)]$ or the boosted $[W_{NM,b}(g_b, n^\star)]$ truncated series. As the asymptotic value $W^{(n_0)}_{NM,\infty}$ we take the hypergeometric sum (32) with $n_0 = 4$ computed at the chosen $g^2 = 6/\beta = 1$. Even though part of the decrease in the boosted coefficients is "eaten" up by the fact that $g^2_b(= 1.6832) > g^2(= 1)$, we see that the boosted series is clearly superior. For example, for W_{11} we have a truncation error $\sim 10^{-3}$ at 10th order in the boosted series, but we would have to go nearly to the 30th order in naive perturbation theory to achieve the same accuracy.

Figure 15 suggests that using the naive perturbative series for $W_{11,\rm hyp}(g, n^\star)$ in (40) to compute g^2_b for a given g^2 is a poor choice. A much better convergence towards the total perturbative plaquette is obtained by using the coefficients $W^{(n)}_{11,b,\rm hyp}$. This suggests to define the boosted coupling $g^2_b(g^2)$ by solving the implicit equation

$$g^2_b = \frac{g^2}{W_{11,b,\rm hyp}(g_b, n^\star)}, \tag{46}$$

where

$$W_{11,b,\rm hyp}(g_b, n^\star) = 1 + \sum_{n=1}^{n^\star} W^{(n)}_{11,b,\rm hyp} g^{2n}_b. \tag{47}$$

One essential justification for choosing (46) is the behavior of the perturbative series of a Wilson loop for large

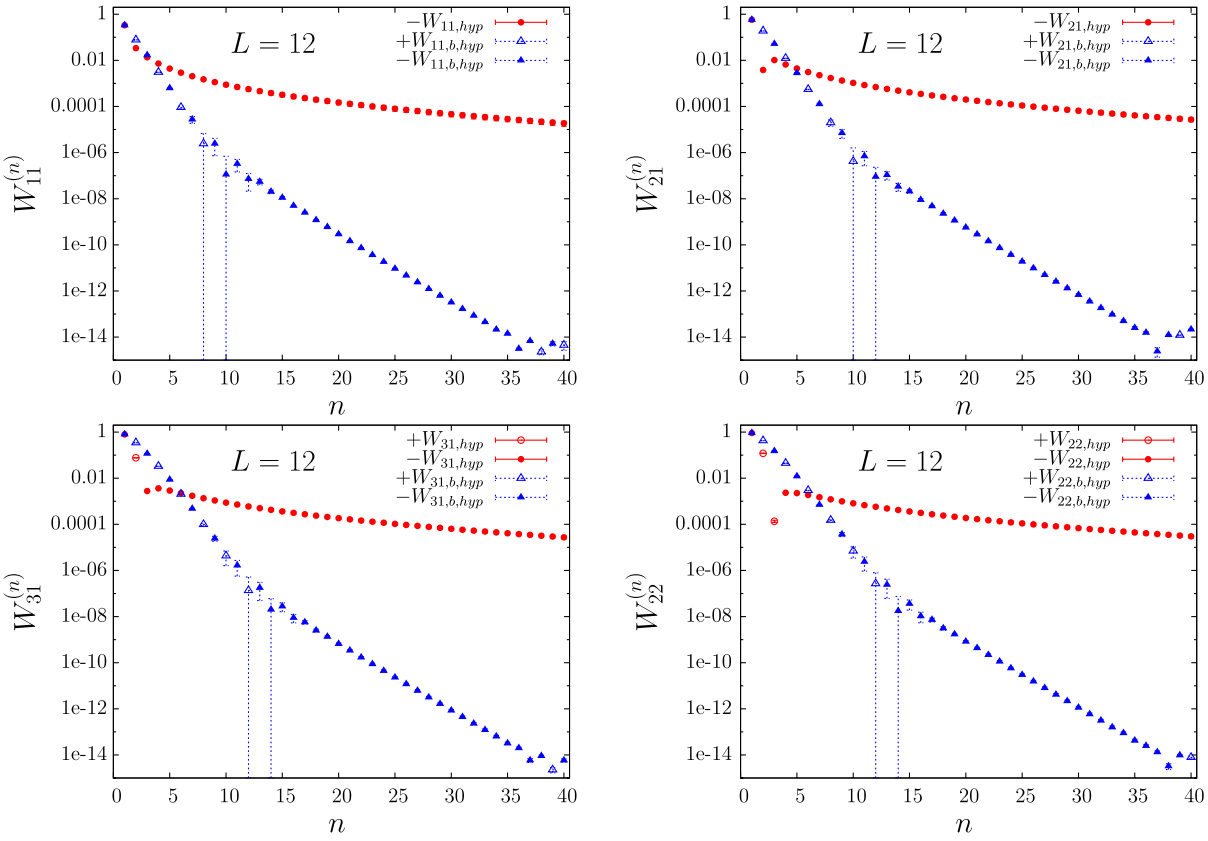

FIG. 14 (color online). Coefficients for the naive and boosted series based on the hypergeometric model for W_{11}, W_{21}, W_{31} and W_{22} as function of the loop order n.

β (small g^2) in comparison to the nonperturbative measurement: in this coupling range the Wilson loop should be dominated by the perturbative content. We introduce the relative difference

$$\tilde{W}_{NM}(\beta) - 1 = \frac{W_{NM,\mathrm{PT}}(\beta) - W_{NM,\mathrm{MC}}(\beta)}{W_{NM,\mathrm{MC}}(\beta)}. \qquad (48)$$

where the index "PT" stands for the perturbative value of the Wilson loop and "MC" denotes the Monte Carlo result. This quantity should tend to zero for large β. In Fig. 16 we plot $\tilde{W}_{11}(\beta) - 1$ as function of β. The β dependence clearly shows that the boosted coupling computed from (46) gives the best behavior for the small g^2 where the plaquette from that perturbative series practically

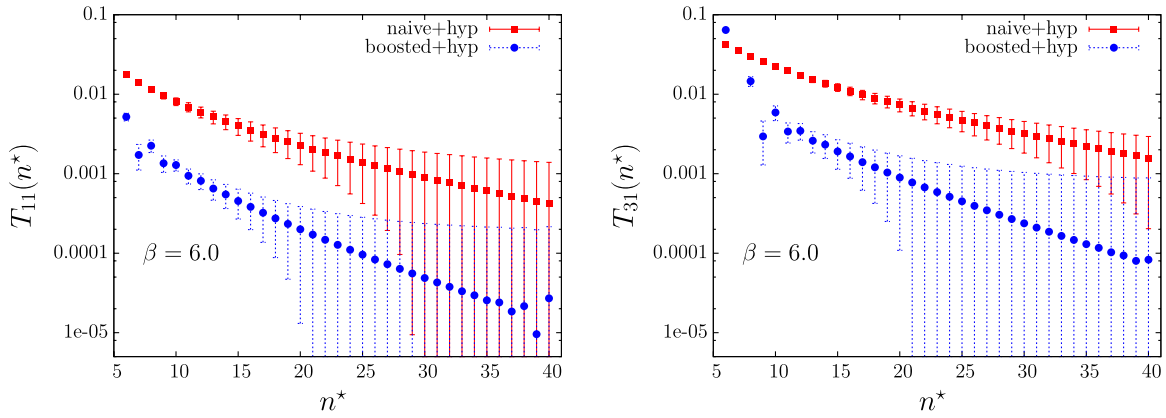

FIG. 15 (color online). Truncation errors $T_{NM}(n^\star)$ (45) for W_{11} (left panel) and W_{31} (right panel) at $L = 12$ and $\beta = 6$ using the naive and the boosted series on the basis of the hypergeometric model. The hypergeometric model values for the total sum are $W_{11,\infty}^{(n_0=4)} = 0.59409(8)$ and $W_{31,\infty}^{(n_0=4)} = 0.25337(22)$.

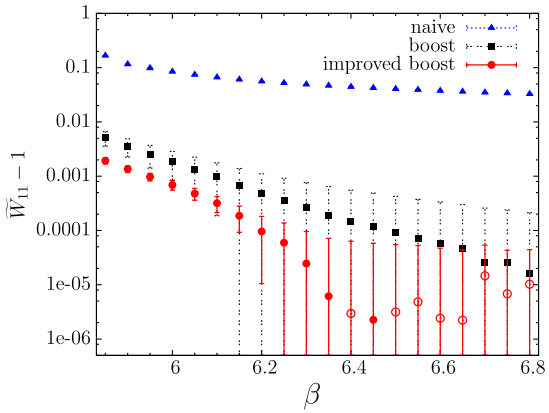

FIG. 16 (color online). $\tilde{W}_{11}(\beta) - 1$ as function of $\beta = 6/g^2$ for $n^\star = 20$, "naive" with $W_{11,\mathrm{PT}} = W_{11}(g, 20)$; "boost" with $W_{11,\mathrm{PT}} = W_{11,b}(g_b, 20)$ and g_b^2 computed from (40); "improved boost" with $W_{11,\mathrm{PT}} = W_{11,b}(g_b, 20)$ and g_b computed from (46). (Full/open symbols denote positive/negative numbers).

coincides with the Monte Carlo value. Wilson loops with larger loop sizes show a similar behavior.

Note that the definitions of the boosted coupling using either (46) or (40) are calculated from a perturbative input exclusively. Using boosting in standard Monte Carlo measurements, the boosted coupling g_b^2 is defined by dividing the bare coupling squared g^2 by the measured plaquette at given β value. Numerically, this coupling constant behaves in a similar way as that obtained from (46). This is another argument to use expression (46) as definition for the boosted coupling in the perturbation theory.

IV. NONPERTURBATIVE PART OF WILSON LOOPS

A. Reliability of high order lattice perturbation theory

There is much debate to which extent the high order lattice perturbation theory can be trusted and how its results can be used to extract physical quantities. In Ref. [24] the authors have investigated the influence of the finite volume on the possibility of finding infrared renormalons. Using the steepest descent (sd) method, they deduce an upper bound on the order of perturbation theory n^{sd} above which possible infrared effects are tamed for dimension four operators,

$$n < n^{sd} \approx 4\log L + c, \tag{49}$$

where L is the lattice size. However, it is difficult to determine the value of c—in Ref. [24] it was estimated as $c = \mathcal{O}(1)$.

As shown in the preceding Sec. III C we found that the boosted perturbation theory using the raw NSPT coefficients in the range $1 \le n \le 12$ gives already reliable results for the summed series. Furthermore, from the discussion at the end of Sec. II B (see Fig. 6) we feel confident that the finite size effects are under control, which would not be the case if there are infrared effects.

On finite lattices one cannot expect renormalons because of hard ultraviolet ($k < 1/a$) and infrared ($k \ge 2\pi/La$) cutoffs. However, one might expect quadratic and quartic divergences. For the plaquette W_{11} one could write (see, e.g., Ref. [25])

$$W_{11} = C_1(aQ)\langle \mathbb{1} \rangle + C_2(aQ)a^4\langle GG \rangle, \tag{50}$$

with $\langle GG \rangle$ denoting a condensate of dimension four. There could be a mixing between operators $\mathbb{1}$ and GG which would result in an a^4-contribution to C_1,

$$C_1(aQ) = C_1^0(aQ) + C_1^4(aQ)(aQ)^4. \tag{51}$$

The coefficients $C_1^i(aQ)$ themselves diverge at most as powers of $\log(aQ)$. The existence of a quartic divergence would spoil the determination of the condensate. This type of divergence is connected to a pole in the Borel transform of the corresponding, assumed a divergent perturbative series with a factorial growth of the expansion coefficients [26]. We do not observe such a factorial growth up to loop order $n = 20$. This is a fact which we have to accept and appreciate theoretically [27,28].

B. Ratios of Wilson loops

A precise separation of the nonperturbative part of Wilson loops from the corresponding quantities measured on the lattice requires a perturbative computation to very high order. From the discussion in Sec. III C it is clear that the boosted perturbation theory provides an optimal tool for that. We use the version of boosting including the hypergeometric model to smooth the NSPT bare coefficients and go beyond loop order $n = 20$. The boosted coupling is computed from (46) with $n^\star = 40$. Additionally we restrict ourselves to moderate loop sizes which ensures that the boosted coefficients can be determined with sufficient accuracy.

Let us introduce generic ratios of powers of Wilson loops (together with their boosted perturbative expansion) as

$$R^{k,m}_{NM,N'M'} = \frac{(W_{NM})^k}{(W_{N'M'})^m} = \sum_n [R^{k,m}_{NM,N'M'}]^{(n)} g_b^{2n}. \tag{52}$$

In most of the following examples we restrict ourselves to reference loops of size $N' = M' = 1$ (plaquette) and integer powers $k, m > 0$. A generalization to larger N', M' and also to noninteger powers k and m can be easily performed.

We consider now the particular ratios $R^{1,2}_{21,11}$ and $R^{1,3}_{31,11}$. They fulfill the area relation

$$k \times \mathcal{S}_{NM} = m \times \mathcal{S}_{N'M'}, \tag{53}$$

where $\mathcal{S}_{NM}$ is the area of the Wilson loop W_{NM}—in our case of planar rectangular loops we have $\mathcal{S}_{NM} = N \times M$. From considerations of naturalness we would expect the

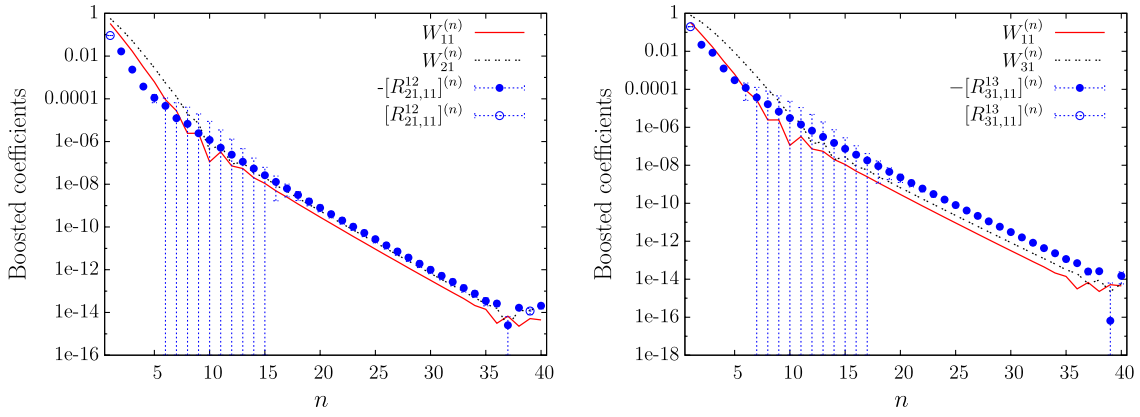

FIG. 17 (color online). Boosted coefficients of ratios (left panel: $[R_{21,11}^{12}]^{(n)}$, right panel: $[R_{31,11}^{13}]^{(n)}$) defined in (52). The thin lines show the corresponding boosted coefficients for the 1×1 and 2×1 (left panel) and 1×1 and 3×1 (right panel) Wilson loops, respectively.

convergence behavior of these types of ratios to be better than other ratios that are not constrained by the area relation (53). We first compare the perturbative coefficients of these ratios with the corresponding coefficients of Wilson loops $W_{NM}^{(n)}$. Figure 17 shows that the coefficients of the ratios behave similar to the coefficients of the Wilson loops (shown for comparison as thin lines without errors) themselves.

Now we define the quantity

$$\Delta_{\mathcal{A}} = \mathcal{A}_{\mathrm{PT}} - \mathcal{A}_{\mathrm{MC}}, \tag{54}$$

where $\Delta_{\mathcal{A}}$ is then the nonperturbative value of the quantity $\mathcal{A}$ and the ratio

$$\tilde{\mathcal{A}} = \frac{\mathcal{A}_{\mathrm{PT}}}{\mathcal{A}_{\mathrm{MC}}}. \tag{55}$$

In the case of Wilson loops $\Delta_{\mathcal{A}} > 0$ and $\Delta_{\mathcal{A}} \ll \mathcal{A}_{\mathrm{PT}}$. Since we know the nonperturbative piece to be much smaller than the perturbative one we can expand $\tilde{\mathcal{A}}$ in powers of $\Delta_{\mathcal{A}}$. To first order we have

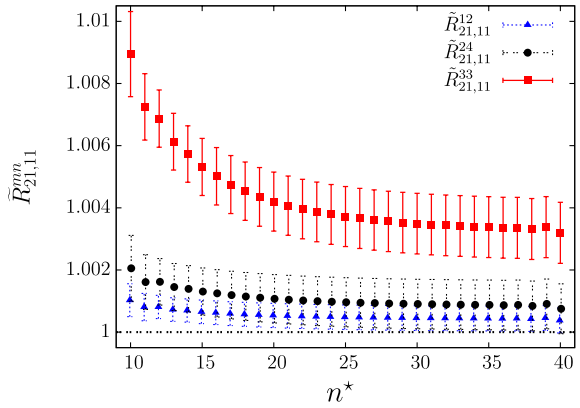

FIG. 18 (color online). $\tilde{R}_{21,11}^{k,m}$ for $(k, m) = (1, 2)$ (2, 4) and (3, 3) as function of loop order $n^\star$ up to which the ratio is summed up.

$$\tilde{\mathcal{A}} \simeq 1 + \frac{\Delta_{\mathcal{A}}}{\mathcal{A}_{\mathrm{PT}}}. \tag{56}$$

Applying this expansion taking in place of $\tilde{\mathcal{A}}$ the ratios $\tilde{R}$ for the R introduced in (52) we have

$$\tilde{R}_{NM,N'M'}^{k,m} \simeq 1 + k\frac{\Delta_{W_{NM}}}{W_{NM,\mathrm{PT}}} - m\frac{\Delta_{W_{N'M'}}}{W_{N'M',\mathrm{PT}}}. \tag{57}$$

In Fig. 18 we show an example for some ratios $\tilde{R}_{NM,N'M'}^{k,m}$ at $\beta = 6$. We have used our own Monte Carlo measurements of Wilson loops generated at the same lattice size [29]. One recognizes that for large $n^\star$ the ratios tend to $\tilde{R}_{NM,N'M'}^{k,m} \simeq 1$. For smaller powers m and k this behavior is more pronounced. Additionally, one finds that the "non-natural" choice $(k, m) = (3, 3)$ leads to a significantly different behavior. Thus, Fig. 18 strongly suggests to use powers (k, m) which obey the area relation (53).

Using for A in the $\tilde{A}$ definition (55) the quantity $R_{NM,N'M'}^{k,m}$ (52) one can easily derive a formula to determine the "deviation from perturbation theory," $\Delta_{W_{NM}}$, for a $N \times M$ Wilson loop as

$$\Delta_{W_{NM}}(W_{N'M'}) = \left[1 - \exp\left(-\frac{d}{dk}\log(\tilde{R}_{NM,N'M'}^{k,m})\right)\right] W_{NM,\mathrm{PT}}, \tag{58}$$

where we made explicit the dependence of $\Delta_{W_{NM}}$ on the reference loop $W_{N'M'}$. Values of (N, M, k) and $(N'M', m)$ are related by (53). Inserting the boosted perturbative series for $W_{NM,\mathrm{PT}}$ and the Monte Carlo measured values $W_{NM,\mathrm{MC}}$ for various values of the inverse coupling β into (58) one obtains rather easily the desired a dependent nonperturbative part $\Delta_{W_{NM}}(a)$ of W_{NM} upon using the known function $\beta(a)$.

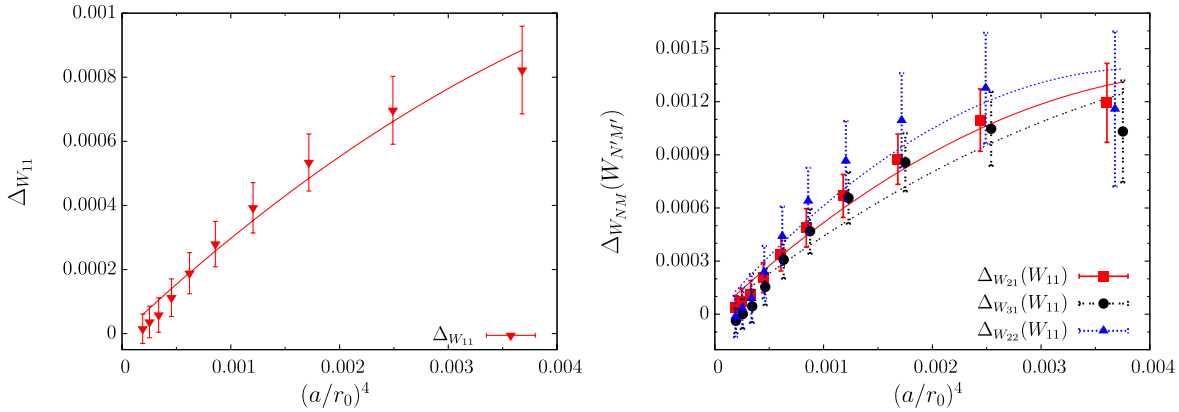

FIG. 19 (color online). $\Delta_{W_{11}}$ (left panel) and $\Delta_{W_{NM}}$ (right panel) as function of a^4 together with their corresponding fits assuming a^4 and $(a^4)^2$ contributions.

C. Condensate of dimension four on the lattice

One special case of the nonperturbative part of Wilson loops is $\Delta_{W_{11}} = W_{11,\mathrm{PT}} - W_{11,\mathrm{MC}}$ which is directly connected to the gluon condensate introduced in Ref. [1]. There is a commonly used relation between the Monte Carlo measured plaquette and its perturbative counterpart,

$$W_{11,\mathrm{MC}} = W_{11,\mathrm{PT}} - a^4 \frac{\pi^2}{36}\left(\frac{-b_0 g^3}{\beta(g)}\right)\left\langle \frac{\alpha}{\pi} GG \right\rangle, \qquad (59)$$

which defines the gluon condensate $\langle \frac{\alpha}{\pi} GG \rangle$ on the lattice.[2] In contrast to (58), relation (59) allows us to determine the gluon condensate from the 1×1 Wilson loop only. An alternative could be to find $\Delta_{W_{11}}$ from (58) choosing a suitable reference Wilson loop. As discussed in Sec. IV A this is strictly valid only in the absence of renormalon ambiguities which is assumed to be the case in the following.

In (59) it is assumed that there is only a single, nonperturbative quantity of dimension four contributing to the plaquette. It has been speculated [30] that in the difference between the perturbative and the lattice Monte Carlo plaquette also an a^2 contribution might be present. That difference depends on $n^\star$ denoting the truncation of the perturbative series as expressed by the $n^\star$ dependence of the corresponding coefficients,

$$\begin{aligned}\Delta_{W_{11}}(n^\star) &= W_{11,\mathrm{PT}}(n^\star) - W_{11,\mathrm{MC}} \\ &= c_2(n^\star)a^2 + c_4(n^\star)a^4. \end{aligned} \qquad (60)$$

In Ref. [11] Narison and Zakharov have presented arguments that a nonzero value of the coefficient $c_2(n^\star)$ is an artifact due to the truncation—above some value of $n^\star$ that coefficient should vanish.

[2] In (59) $\beta(g)$ denotes the standard β-function with b_0 being its leading coefficient.

For the estimate of the gluon condensate we are in the position to take the most precise perturbative values available—in our computation these are the summed series based on hypergeometric functions ($n^\star \to \infty$) given in (34) with the parameters of Table III. So we can ask the question, whether there is a significant a^2 dependence for the nonperturbative parts $\Delta_{W_{NM}}$ derived from (58) making a corresponding ansatz as in (60).

To find the dependence of the nonperturbative part on the lattice spacing a, we consider the lattice coupling region $\beta_{\min} \le \beta \le \beta_{\max}$. $\beta_{\min} = 5.85$ is determined by the convergence radius of the perturbative series. In the analysis we have used nonperturbative Wilson loops from the same lattice size as the largest NSPT lattice and have chosen $\beta_{\max} = 6.3$. To relate the different lattice couplings β to a/r_0, where r_0 is the Sommer scale, we use Ref. [31].

In the left panel of Fig. 19 we show $\Delta W_{11}(a)$ as function of a^4. One observes that there is not much room for an additional a^2 dependence. On the other hand, we find a significant bending for larger $a(g^2)$ which can be parametrized as an $(a^4)^2$ correction term. This might be a sign of breaking scaling on the coarsest lattices, or it could be the signature of higher dimensional condensates considered in Ref. [32]. That correction is relatively small for $\Delta_{W_{11}}$. For larger Wilson loops we find this deviation from a pure a^4 dependence more pronounced as shown in the right of Fig. 19. We should mention that, using the summed perturbative series of the hypergeometric model, the nonperturbative parts $\Delta_{W_{NM}}$ are independent of the choice of the reference loops [as indicated in (58)] and also agree for the plaquette case with the simple subtraction scheme (59).

In Fig. 20 we plot $c_4(n^\star)$ for various Wilson loops. One recognizes a pronounced plateau for $n^\star > 30$. In Table V we give the values of the coefficients c_4 both for the boosted series summed up to $n^\star = 40$ and as obtained from the infinite series, respectively. On dimensional grounds one would expect that c_4 would be approximately proportional to the square of the Wilson loop area [32].

TABLE V. Coefficients c_4 for the Wilson loops W_{NM} obtained from the boosted perturbation theory up to $n^\star = 40$ and from the series summed to infinity using the hypergeometric model.

	c_4 from boosting ($n^\star = 40$)	c_4 from the hypergeometric model
W_{11}	0.30(3)	0.31(3)
W_{21}	0.54(5)	0.56(5)
W_{31}	0.47(9)	0.49(10)
W_{22}	0.67(10)	0.70(11)

TABLE VI. Gluon condensate at $L = 12$ ($r_0 = 0.5$ fm).

	$r_0^4\langle\frac{\alpha}{\pi}GG\rangle$	$\langle\frac{\alpha}{\pi}GG\rangle$ [GeV^4]
$\Delta_{W_{11}}$	1.16(12)	0.028(3)

From Table V we do see an increase in c_4, but it is much slower than area squared (in fact the a^4 term in the 3×1 loop is smaller than the 2×1 loop, though the error bars overlap).

Introducing the Sommer scale r_0, a physical value for the condensate can be extracted from the coefficient c_4. If we approximate $(\frac{-b_0 g^3}{\beta(g)}) \sim 1$ in (59), we extract from $\Delta_{W_{11}}$ the gluon condensate as given in Table VI. This value is slightly lower than the value 0.04(1) GeV^4 found in Ref. [8]. The main reason for the difference is that in Ref. [8] the boosted series was truncated at $n^\star = 12$, while in the present work we make an estimate of the contribution from higher terms in the boosted series.

V. SUMMARY

In this paper we presented the result of NSPT calculations for Wilson loops of various sizes using the Wilson gauge action. Within the framework of NSPT we were able to determine the perturbative coefficients of those loops up to loop order $n = 20$ for different lattice sizes as numerically clear signals.

Up to that order we did not observe signs of a factorial n dependence as expected for an asymptotic series. Assuming that this behavior is not spoiled at larger n, we were able to describe the n dependence of the series by a simple recursion relating subsequent orders. Solving that relation, the sum over all orders has been represented by a hypergeometric function. Its branch cut discontinuity defines a convergence radius of the series at positive g^2.

Using the naive perturbative series of the Wilson loops in the bare coupling squared $g^2 = 6/\beta$, the summed series up to $n^\star$ converges only slowly to some asymptotic value. This has led us to apply boosting-a rearrangement of the perturbative series in terms of the so-called boosted coupling as expansion parameter where we expect that the summed series reaches a stable plateau already after moderate loop orders. For moderate Wilson loop sizes these plateaus have been found.

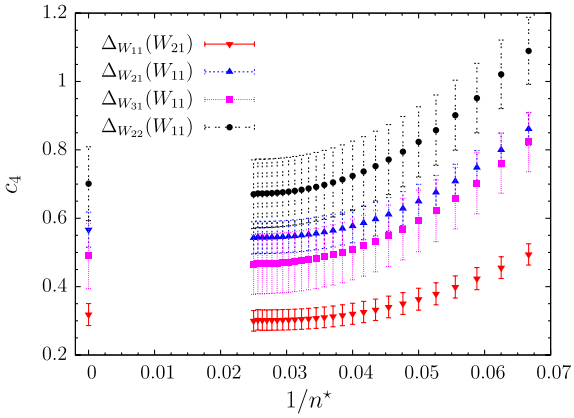

FIG. 20 (color online). Coefficient c_4 as function of the inverse loop order $1/n^\star$ for different Wilson loops. The data points at "$1/n^\star = 0$" represent the series summed to infinity using the hypergeometric model.

The transformation from the naive perturbative series to the boosted series is numerically delicate, involving large cancellations. Simply transforming the NSPT raw expansion coefficients leads to very noisy boosted coefficients beyond $n \approx 8$. To get around this problem we "smoothed" the coefficients of the naive perturbative series using the presented hypergeometric model before calculating the boosted series. The resulting smoothed boosted coefficients are much more stable, and this strongly suggests that the observed rapid falloff of the boosted coefficients continues to large loop orders.

We introduced ratios of powers of Wilson loops which then have been treated within boosted perturbation theory. In many cases the truncation errors for these ratios are much smaller than the truncation errors for the Wilson loops themselves.

The results of the boosted perturbative series are extremely close to the Monte Carlo values of the Wilson loops; the same applies to their ratios. For $\beta > 6$ ($g^2 < 1$) the differences are typically in the third or fourth decimal place. Looking at the small deviations between Monte Carlo results and boosted perturbation theory allows for a determination of the nonperturbative parts of Wilson loops. We find that the dominant behavior of the nonperturbative part scales like a^4.

As a special case we have calculated the gluon condensate $\langle\frac{\alpha}{\pi}GG\rangle$ from the plaquette. The found number is somewhat larger than that in the phenomenological Shifman-Vainshtein-Zakharov sum rule approach [1]-at least for our 12^4 lattice. Our number agrees within errors with the estimate $\langle\frac{\alpha}{\pi}GG\rangle = 0.024(8)$ GeV^4 presented by Narison in Ref. [33] which is based on a study of heavy quarkonia mass splittings.

We have checked the regularly reappearing claim, that the Wilson loop has, in addition to its "canonical" a^4 dependence, a significant part showing an a^2 power dependence. Our results show that in the chosen β-region the

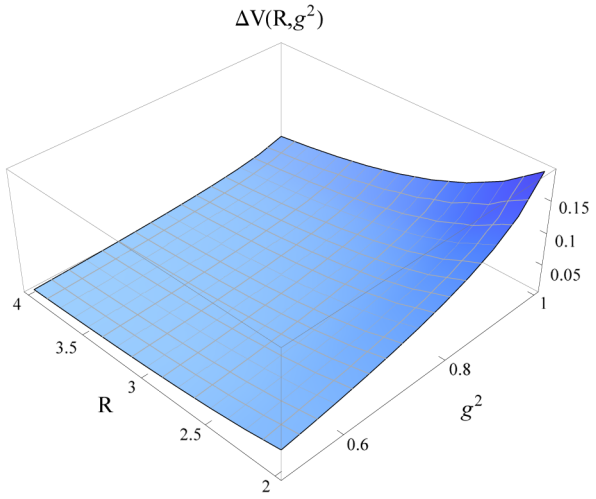

FIG. 21 (color online). The perturbative potential difference ΔV obtained from the perturbative Wilson loops up to loop order 20 as a function of the distance R and g^2.

nonperturbative parts of the Wilson loops W_{NM} can be well described by an a^4 ansatz with an $(a^4)^2$ correction term. For the difference between the perturbative and the lattice Monte Carlo plaquette $\Delta_{W_{11}}$ this correction is rather small.

If infinite or large order perturbation theory was to reflect the long distance properties of QCD, we would expect the Wilson loops to show an area-law behavior and the static potential to grow linearly with distance. As a result, the Borel transform would exhibit a pole at $1/b_0 = 16\pi^2/11$, and the coefficients of the perturbative series should show a factorial growth. (Then, for comparison, the gluon condensate would show up as a pole at $2/b_0 = 32\pi^2/11$.) Instead, we find

$$W(R, T) \propto \frac{T}{R}, \tag{61}$$

for $R = 2, 3, 4$ and $T = 5$, within a few percent, and no sign of an infrared renormalon.[3] This result holds for all couplings within the radius of convergence of the perturbative series, $0 < g^2 \lesssim 1.1$.

In Fig. 21 we show the potential difference ΔV as function of R and g^2 calculated from the series variant of the Creutz ratio

$$\Delta V(R) = V(R-1) - V(R) = \log\frac{W(R, T)W(R-1, T-1)}{W(R, T-1)W(R-1, T)}, \tag{62}$$

using the perturbative Wilson loops up to loop order 20. For a linearly increasing potential one would expect ΔV to be a constant proportional to the string tension. In fact, ΔV decreases with R for all g^2 within the radius of convergence consistent with the expected Coulomb behavior $1/(R(R-1))$.

A look at the β-function suggests, furthermore, that the perturbative theory is separated from the strong coupling phase through a pole, similar to the supersymmetric Yang-Mills theory [36], indicating that there is no direct contradiction with the strong coupling expansion. A similar result to (61) was found in Monte Carlo simulations of gauge fixed noncompact lattice QCD [37,38], which took into account only small fluctuations of the gauge fields.

This leads us to conclude-on the basis of our present results, *nota bene*-that the perturbative series carry no information on the confining properties of the theory and the nontrivial features of the QCD vacuum. The positive aspect of this result is that the perturbative tail can be cleanly separated from the Monte Carlo results for the plaquette.

[3]We have nothing to add to Ref. [34] and to the argument of Ref. [35] that there is no physical significance to these ambiguities.

ACKNOWLEDGMENTS

This investigation has been supported partly by DFG under Contract No. SCHI 422/8-1 and by the EU Grant No. 227431 (Hadron Physics2). R. M. is supported by the Research Executive Agency (REA) of the European Union under Grant No. PITN-GA-2009-238353 (ITN STRONGnet). We thank the RCNP at Osaka University for providing computer resources.

APPENDIX

We present in Tables VII, VIII, IX, X, XI, XII, and XIII all considered rectangular perturbative Wilson loops of

TABLE VII. Perturbative coefficients for $L = 4$.

n	$W_{11}^{(n)}$	$W_{21}^{(n)}$	$W_{22}^{(n)}$
1	−0.332147(22)	−0.567064(34)	−0.874683(122)
2	−0.033411(15)	−0.004571(25)	0.104041(63)
3	−0.013368(13)	−0.010094(28)	−0.000735(58)
4	−0.006983(1)	−0.006394(13)	−0.002683(12)
5	−0.004179(8)	−0.004167(9)	−0.002284(1)
6	−0.002719(6)	−0.002859(8)	−0.001777(9)
7	−0.001872(6)	−0.002041(8)	−0.001368(1)
8	−0.001342(5)	−0.001503(8)	−0.001063(9)
9	−0.000992(5)	−0.001134(7)	−0.000834(8)
10	−0.000752(4)	−0.000874(6)	−0.000663(7)
11	−0.000581(4)	−0.000684(5)	−0.000534(6)
12	−0.000456(4)	−0.000544(5)	−0.000433(6)
13	−0.000363(3)	−0.000437(4)	−0.000355(6)
14	−0.000292(3)	−0.000355(4)	−0.000293(6)
15	−0.000238(3)	−0.000291(4)	−0.000243(5)
16	−0.000195(2)	−0.000240(4)	−0.000204(5)
17	−0.000161(2)	−0.000200(3)	−0.000171(5)
18	−0.000134(2)	−0.000167(3)	−0.000145(5)
19	−0.000112(2)	−0.000141(3)	−0.000123(4)
20	−0.000094(2)	−0.000119(3)	−0.000105(4)

TABLE VIII. Perturbative coefficients for $L = 6$.

n	$W_{11}^{(n)}$	$W_{21}^{(n)}$	$W_{22}^{(n)}$	$W_{31}^{(n)}$	$W_{32}^{(n)}$	$W_{33}^{(n)}$
1	−0.333112(15)	−0.573644(44)	−0.907518(112)	−0.798086(71)	−1.193307(174)	−1.500876(291)
2	−0.033829(6)	−0.003938(26)	0.118297(96)	0.075949(52)	0.313019(171)	0.609060(335)
3	−0.013641(4)	−0.010199(9)	0.000024(16)	−0.002820(12)	−0.005402(37)	−0.050954(108)
4	−0.007202(2)	−0.006571(5)	−0.002375(9)	−0.003622(3)	−0.000139(18)	−0.000273(38)
5	−0.004366(3)	−0.004366(6)	−0.002227(12)	−0.002878(6)	−0.000573(8)	−0.000083(34)
6	−0.002881(4)	−0.003047(7)	−0.001813(12)	−0.002190(8)	−0.000684(1)	−0.000138(7)
7	−0.002014(4)	−0.002214(7)	−0.001440(12)	−0.001675(8)	−0.000629(13)	−0.000147(12)
8	−0.001467(4)	−0.001661(7)	−0.001151(12)	−0.001303(8)	−0.000551(13)	−0.000156(1)
9	−0.001103(4)	−0.001278(6)	−0.000927(1)	−0.001028(7)	−0.000473(1)	−0.000157(8)
10	−0.000850(3)	−0.001004(5)	−0.000755(8)	−0.000824(6)	−0.000404(8)	−0.000150(7)
11	−0.000669(3)	−0.000802(4)	−0.000622(6)	−0.000670(5)	−0.000346(6)	−0.000139(6)
12	−0.000535(3)	−0.000650(3)	−0.000518(4)	−0.000551(4)	−0.000298(4)	−0.000126(5)
13	−0.000434(2)	−0.000533(3)	−0.000435(3)	−0.000458(3)	−0.000257(2)	−0.000114(5)
14	−0.000356(2)	−0.000442(2)	−0.000368(2)	−0.000384(2)	−0.000222(2)	−0.000102(4)
15	−0.000295(2)	−0.000370(2)	−0.000313(2)	−0.000324(2)	−0.000192(2)	−0.000091(4)
16	−0.000247(2)	−0.000312(2)	−0.000268(2)	−0.000276(2)	−0.000167(2)	−0.000080(3)
17	−0.000208(2)	−0.000265(2)	−0.000231(2)	−0.000236(2)	−0.000145(2)	−0.000071(3)
18	−0.000177(2)	−0.000227(2)	−0.000200(2)	−0.000203(2)	−0.000127(2)	−0.000063(2)
19	−0.000151(2)	−0.000195(2)	−0.000173(2)	−0.000175(2)	−0.000111(2)	−0.000056(2)
20	−0.000130(1)	−0.000169(2)	−0.000151(2)	−0.000152(2)	−0.000098(2)	−0.000050(2)

sizes $N \times M$ with $N, M = 1, \ldots, L/2$ for different sizes L of the used hypercubic lattices L^4 in the form

$$W_{NM} = 1 + \sum_{n=1}^{20} W_{NM}^{(n)} g^{2n}. \tag{A1}$$

The expansion coefficients $W_{NM}^{(n)}$ are the result of the extrapolation to zero Langevin step size using (17). The reported errors are the fit errors from the extrapolation $\varepsilon \to 0$. The presented numbers for larger Wilson loops and higher loop orders are collected irrespective of possible problems with the signal to noise ratio at a given order n as discussed in Sec. II B and have to be taken with care. In Table XIV we give some perturbative Wilson loops as result of an infinite series using the described

TABLE IX. Perturbative coefficients for $L = 8$.

n	$W_{11}^{(n)}$	$W_{21}^{(n)}$	$W_{22}^{(n)}$	$W_{31}^{(n)}$	$W_{41}^{(n)}$
1	−0.333236(8)	−0.574473(16)	−0.911469(27)	−0.800665(29)	−1.023410(49)
2	−0.033852(5)	−0.003818(8)	0.119976(19)	0.076987(16)	0.206839(26)
3	−0.013670(3)	−0.010214(4)	0.000196(7)	−0.002770(7)	−0.002536(14)
4	−0.007229(3)	−0.006594(4)	−0.002321(9)	−0.003628(5)	−0.001501(7)
5	−0.004389(2)	−0.004397(4)	−0.002243(5)	−0.002892(6)	−0.001525(6)
6	−0.002903(2)	−0.003080(3)	−0.001845(5)	−0.002209(5)	−0.001309(6)
7	−0.002034(2)	−0.002246(2)	−0.001478(5)	−0.001697(3)	−0.001076(4)
8	−0.001487(1)	−0.001693(2)	−0.001194(6)	−0.001328(3)	−0.000880(3)
9	−0.001122(1)	−0.001310(2)	−0.000973(7)	−0.001057(3)	−0.000725(3)
10	−0.000869(1)	−0.001035(3)	−0.000800(7)	−0.000854(3)	−0.000601(3)
11	−0.000687(1)	−0.000832(3)	−0.000664(6)	−0.000700(3)	−0.000502(3)
12	−0.000553(1)	−0.000678(3)	−0.000555(6)	−0.000579(3)	−0.000423(3)
13	−0.000451(2)	−0.000560(3)	−0.000468(5)	−0.000484(3)	−0.000358(3)
14	−0.000372(2)	−0.000467(3)	−0.000398(5)	−0.000408(3)	−0.000306(3)
15	−0.000310(2)	−0.000393(3)	−0.000340(5)	−0.000346(3)	−0.000262(3)
16	−0.000261(2)	−0.000333(3)	−0.000292(5)	−0.000296(3)	−0.000226(3)
17	−0.000221(2)	−0.000284(3)	−0.000252(4)	−0.000254(3)	−0.000195(3)
18	−0.000189(1)	−0.000244(2)	−0.000219(4)	−0.000220(3)	−0.000170(3)
19	−0.000162(1)	−0.000211(2)	−0.000191(4)	−0.000191(3)	−0.000148(3)
20	−0.000140(1)	−0.000183(2)	−0.000167(3)	−0.000167(2)	−0.000130(2)

hypergeometric model for various β values at $L = 12$. In Table XV we collect the values for known loop order coefficients in the infinite volume limit. For W_{11} the first three loop order coefficients are given in [22,23] whereas for the larger Wilson loops only the first two loop orders are known [21]. The first order coefficients can be computed to high precision.

TABLE X. Perturbative coefficients for $L = 8$ (continued).

n	$W_{32}^{(n)}$	$W_{33}^{(n)}$	$W_{42}^{(n)}$	$W_{43}^{(n)}$	$W_{44}^{(n)}$
1	−1.204201(52)	−1.528486(114)	−1.485430(97)	−1.830535(174)	−2.140917(228)
2	0.320661(27)	0.636544(74)	0.595785(62)	1.028662(168)	1.524356(276)
3	−0.005468(14)	−0.055098(20)	−0.048959(22)	−0.174438(58)	−0.396169(154)
4	−0.000135(19)	−0.000547(45)	−0.000495(31)	0.002744(73)	0.025146(116)
5	−0.000592(1)	−0.000131(15)	−0.000219(24)	−0.000108(45)	0.000200(94)
6	−0.000687(12)	−0.000159(28)	−0.000216(20)	−0.000068(44)	0.000011(96)
7	−0.000652(1)	−0.000208(13)	−0.000238(13)	−0.000082(17)	−0.000067(33)
8	−0.000588(1)	−0.000214(17)	−0.000246(11)	−0.000089(14)	−0.000057(28)
9	−0.000514(1)	−0.000196(16)	−0.000233(11)	−0.000077(15)	−0.000027(26)
10	−0.000443(9)	−0.000174(13)	−0.000209(9)	−0.000063(12)	−0.000011(14)
11	−0.000380(7)	−0.000153(1)	−0.000183(7)	−0.000054(8)	−0.000010(7)
12	−0.000326(6)	−0.000136(8)	−0.000160(6)	−0.000048(7)	−0.000013(5)
13	−0.000281(6)	−0.000120(7)	−0.000141(5)	−0.000043(6)	−0.000015(4)
14	−0.000243(5)	−0.000107(7)	−0.000124(5)	−0.000039(5)	−0.000015(4)
15	−0.000210(5)	−0.000095(6)	−0.000109(5)	−0.000035(5)	−0.000013(4)
16	−0.000183(5)	−0.000084(5)	−0.000096(5)	−0.000032(5)	−0.000011(4)
17	−0.000160(5)	−0.000075(5)	−0.000086(5)	−0.000029(4)	−0.000010(4)
18	−0.000141(4)	−0.000068(4)	−0.000076(4)	−0.000027(4)	−0.000009(3)
19	−0.000124(4)	−0.000061(4)	−0.000068(4)	−0.000025(3)	−0.000008(3)
20	−0.000110(4)	−0.000055(4)	−0.000061(4)	−0.000023(3)	−0.000007(2)

TABLE XI. Perturbative coefficients for $L = 12$.

n	$W_{11}^{(n)}$	$W_{21}^{(n)}$	$W_{22}^{(n)}$	$W_{31}^{(n)}$	$W_{41}^{(n)}$	$W_{51}^{(n)}$	$W_{61}^{(n)}$
1	−0.333320(4)	−0.574758(4)	−0.912636(19)	−0.801260(5)	−1.024718(1)	−1.247323(13)	−1.469522(15)
2	−0.033898(1)	−0.003835(2)	0.120423(2)	0.077139(9)	0.207624(22)	0.387381(18)	0.616194(13)
3	−0.013698(3)	−0.010247(5)	0.000136(15)	−0.002788(4)	−0.002610(3)	−0.020698(3)	−0.067876(11)
4	−0.007251(3)	−0.006625(7)	−0.002337(13)	−0.003640(8)	−0.001503(7)	−0.000967(6)	−0.000342(11)
5	−0.004410(3)	−0.004425(6)	−0.002255(11)	−0.002914(9)	−0.001539(1)	−0.000784(1)	−0.000475(6)
6	−0.002922(3)	−0.003106(6)	−0.001861(9)	−0.002233(7)	−0.001326(1)	−0.000724(12)	−0.000406(15)
7	−0.002052(3)	−0.002272(4)	−0.001503(7)	−0.001726(5)	−0.001101(5)	−0.000645(6)	−0.000373(8)
8	−0.001504(2)	−0.001718(3)	−0.001217(4)	−0.001355(3)	−0.000906(3)	−0.000557(4)	−0.000334(6)
9	−0.001138(2)	−0.001333(2)	−0.000994(2)	−0.001082(2)	−0.000748(1)	−0.000475(2)	−0.000289(3)
10	−0.000884(1)	−0.001056(2)	−0.000820(2)	−0.000876(2)	−0.000621(1)	−0.000403(2)	−0.000251(3)
11	−0.000700(1)	−0.000851(1)	−0.000683(3)	−0.000719(2)	−0.000519(2)	−0.000344(2)	−0.000218(3)
12	−0.000565(1)	−0.000696(2)	−0.000574(4)	−0.000597(3)	−0.000438(3)	−0.000295(4)	−0.000191(4)
13	−0.000462(1)	−0.000577(2)	−0.000487(4)	−0.000502(3)	−0.000373(4)	−0.000256(4)	−0.000168(4)
14	−0.000383(1)	−0.000484(2)	−0.000418(4)	−0.000426(3)	−0.000321(4)	−0.000223(4)	−0.000149(3)
15	−0.000320(1)	−0.000409(2)	−0.000361(4)	−0.000364(3)	−0.000278(3)	−0.000196(3)	−0.000132(2)
16	−0.000271(1)	−0.000350(2)	−0.000314(3)	−0.000315(2)	−0.000243(2)	−0.000173(2)	−0.000117(1)
17	−0.000231(1)	−0.000301(2)	−0.000275(2)	−0.000274(2)	−0.000213(2)	−0.000153(2)	−0.000105(1)
18	−0.000199(1)	−0.000261(2)	−0.000242(2)	−0.000239(2)	−0.000188(2)	−0.000136(2)	−0.000094(2)
19	−0.000172(1)	−0.000228(1)	−0.000213(3)	−0.000210(2)	−0.000166(2)	−0.000122(3)	−0.000085(2)
20	−0.000150(1)	−0.000200(1)	−0.000189(3)	−0.000185(2)	−0.000147(3)	−0.000109(3)	−0.000077(2)

TABLE XII. Perturbative coefficients for $L = 12$ (continued).

n	$W_{32}^{(n)}$	$W_{33}^{(n)}$	$W_{42}^{(n)}$	$W_{43}^{(n)}$	$W_{44}^{(n)}$	$W_{52}^{(n)}$	$W_{53}^{(n)}$
1	−1.207005(31)	−1.535522(52)	−1.491384(41)	−1.845142(72)	−2.170005(100)	−1.772698(66)	−2.148586(117)
2	0.322694(4)	0.643882(9)	0.601963(23)	1.048051(37)	1.571598(94)	0.958407(28)	1.538376(110)
3	−0.005740(18)	−0.056823(24)	−0.050320(9)	−0.181032(13)	−0.418636(81)	−0.155201(16)	−0.404144(11)
4	−0.000112(19)	−0.000446(44)	−0.000514(12)	0.003334(36)	0.028597(70)	0.002475(12)	0.027039(50)
5	−0.000592(11)	−0.000136(15)	−0.000182(2)	−0.000224(12)	−0.000196(13)	−0.000188(19)	−0.000207(18)
6	−0.000685(9)	−0.000113(15)	−0.000197(8)	−0.000059(18)	−0.000019(16)	0.000109(14)	−0.000003(30)
7	−0.000663(7)	−0.000178(12)	−0.000241(6)	−0.000074(13)	−0.000064(18)	−0.000103(9)	−0.000054(20)
8	−0.000598(4)	−0.000196(5)	−0.000248(4)	−0.000074(11)	−0.000031(14)	−0.000108(8)	−0.000043(20)
9	−0.000523(2)	−0.000192(5)	−0.000234(5)	−0.000067(9)	−0.000024(4)	−0.000101(9)	−0.000027(11)
10	−0.000453(3)	−0.000177(3)	−0.000210(3)	−0.000059(1)	−0.000013(8)	−0.000090(6)	−0.000015(8)
11	−0.000391(5)	−0.000161(7)	−0.000188(6)	−0.000056(8)	−0.000015(11)	−0.000083(6)	−0.000018(14)
12	−0.000339(6)	−0.000148(9)	−0.000170(7)	−0.000058(11)	−0.000023(7)	−0.000079(6)	−0.000025(12)
13	−0.000297(6)	−0.000137(9)	−0.000155(7)	−0.000059(8)	−0.000029(5)	−0.000076(5)	−0.000028(7)
14	−0.000261(5)	−0.000126(7)	−0.000141(5)	−0.000058(5)	−0.000030(5)	−0.000071(3)	−0.000029(4)
15	−0.000230(4)	−0.000116(5)	−0.000128(3)	−0.000055(4)	−0.000026(8)	−0.000067(2)	−0.000026(6)
16	−0.000204(3)	−0.000106(5)	−0.000116(3)	−0.000051(6)	−0.000023(11)	−0.000061(3)	−0.000023(8)
17	−0.000182(3)	−0.000096(7)	−0.000105(4)	−0.000047(8)	−0.000020(12)	−0.000056(5)	−0.000021(9)
18	−0.000162(4)	−0.000087(8)	−0.000095(5)	−0.000043(9)	−0.000018(11)	−0.000052(5)	−0.000020(9)
19	−0.000145(5)	−0.000078(9)	−0.000086(6)	−0.000040(9)	−0.000017(9)	−0.000047(6)	−0.000020(8)
20	−0.000130(5)	−0.000071(9)	−0.000077(6)	−0.000037(8)	−0.000016(6)	−0.000043(5)	−0.000018(6)

TABLE XIII. Perturbative coefficients for $L = 12$ (continued).

n	$W_{54}^{(n)}$	$W_{55}^{(n)}$	$W_{62}^{(n)}$	$W_{63}^{(n)}$	$W_{64}^{(n)}$	$W_{65}^{(n)}$	$W_{66}^{(n)}$
1	−2.484945(156)	−2.807271(225)	−2.052506(78)	−2.448879(142)	−2.794661(184)	−3.121967(258)	−3.438947(291)
2	2.181680(181)	2.906812(327)	1.391688(52)	2.114904(186)	2.879504(270)	3.716609(450)	4.631615(573)
3	−0.790329(77)	−1.342663(185)	−0.341621(19)	−0.751605(84)	−1.322744(141)	−2.086833(280)	−3.069039(366)
4	0.101235(36)	0.260769(172)	0.020658(33)	0.093854(31)	0.255213(42)	0.548424(285)	1.025063(600)
5	−0.002457(18)	−0.015589(148)	−0.000052(25)	−0.002038(23)	−0.015007(49)	−0.056854(283)	−0.156497(515)
6	0.000160(35)	0.000420(19)	−0.000080(18)	0.000078(14)	0.000253(48)	0.001978(79)	0.008403(118)
7	−0.000078(29)	−0.000175(44)	−0.000076(11)	−0.000051(12)	−0.000048(49)	−0.000388(108)	−0.000301(267)
8	−0.000020(16)	−0.000011(8)	−0.000059(11)	−0.000045(23)	−0.000034(33)	0.000034(26)	−0.000051(119)
9	−0.000008(6)	0.000015(11)	−0.000049(9)	−0.000022(1)	−0.000009(25)	−0.000004(50)	0.000008(124)
10	0.000007(12)	0.000030(16)	−0.000037(4)	0.000003(1)	0.000015(17)	0.000056(16)	0.000093(31)
11	−0.000005(12)	0.000008(1)	−0.000035(3)	0.000002(17)	−0.000004(1)	−0.000014(7)	−0.000066(26)
12	−0.000016(6)	−0.000002(2)	−0.000037(5)	−0.000005(11)	−0.000011(4)	−0.000022(9)	−0.000049(5)
13	−0.000020(4)	−0.000006(1)	−0.000038(3)	−0.000012(5)	−0.000013(11)	−0.000010(9)	−0.000026(17)
14	−0.000019(6)	−0.000008(3)	−0.000038(1)	−0.000016(5)	−0.000009(11)	−0.000004(8)	0.000002(22)
15	−0.000015(8)	−0.000007(6)	−0.000036(2)	−0.000016(5)	−0.000004(9)	−0.000001(7)	0.000012(11)
16	−0.000010(1)	−0.000005(8)	−0.000033(3)	−0.000015(6)	−0.000002(7)	0.000000(6)	0.000014(3)
17	−0.000008(1)	−0.000004(9)	−0.000030(5)	−0.000013(7)	−0.000001(6)	0.000000(5)	0.000009(5)
18	−0.000007(8)	−0.000003(7)	−0.000028(5)	−0.000012(6)	0.000000(5)	−0.000001(4)	0.000002(4)
19	−0.000007(6)	−0.000003(5)	−0.000025(5)	−0.000011(5)	0.000000(3)	−0.000002(3)	−0.000002(3)
20	−0.000006(4)	−0.000002(3)	−0.000023(4)	−0.000010(4)	0.000000(2)	−0.000002(2)	−0.000004(5)

TABLE XIV. Summed series of perturbative Wilson loops at $L = 12$ using the described hypergeometric model as function of β.

β	W_{11}^{∞}	W_{21}^{∞}	W_{31}^{∞}	W_{22}^{∞}
5.85	0.57595(14)	0.36021(22)	0.22936(28)	0.16659(41)
5.9	0.58254(11)	0.36901(16)	0.23814(21)	0.17557(29)
5.95	0.588518(92)	0.37692(13)	0.24602(17)	0.18354(24)
6	0.594092(80)	0.38429(11)	0.25337(14)	0.19095(20)
6.05	0.599358(71)	0.39125(10)	0.26034(12)	0.19797(17)
6.1	0.604372(63)	0.397894(90)	0.26702(11)	0.20469(15)
6.15	0.609172(57)	0.404260(81)	0.273454(99)	0.21118(14)
6.2	0.613784(52)	0.410391(75)	0.279676(89)	0.21745(12)
6.25	0.618228(48)	0.416313(67)	0.285714(81)	0.22355(11)
6.3	0.622521(44)	0.422047(62)	0.291587(74)	0.22949(10)
6.35	0.626675(41)	0.427612(57)	0.297310(68)	0.235295(94)
6.4	0.630703(38)	0.433020(53)	0.302895(63)	0.240961(87)
6.45	0.634612(35)	0.438283(49)	0.308354(58)	0.246508(80)
6.5	0.638412(33)	0.443412(45)	0.313694(54)	0.251941(75)
6.55	0.642108(31)	0.448415(44)	0.318922(50)	0.257270(70)
6.6	0.645708(29)	0.453299(40)	0.324046(47)	0.262499(65)
6.65	0.649216(27)	0.458071(37)	0.329071(44)	0.267634(61)
6.7	0.652637(25)	0.462737(35)	0.334001(41)	0.272680(57)
6.75	0.655977(23)	0.467302(33)	0.338842(39)	0.277641(54)
6.8	0.659239(22)	0.471771(31)	0.343596(36)	0.282521(50)

TABLE XV. Coefficients of lowest loop orders in the infinite volume limit.

W_{NM}	$W_{NM,\infty}^{(1)}$	$W_{NM,\infty}^{(2)}$	$W_{NM,\infty}^{(3)}$
W_{11} [22,23]	$-1/3$	$-0.0339109931(3)$	$-0.0137063(2)$
W_{21} [21]	-0.57483367	$-0.003857(17)$	
W_{31} [21]	-0.80146372	0.07717(5)	
W_{22} [21]	-0.91287436	0.12040(7)	

[1] M. A. Shifman, A. I. Vainshtein, and V. I. Zakharov, Nucl. Phys. **B147**, 385 (1979).
[2] T. Banks, R. Horsley, H. R. Rubinstein, and U. Wolff, Nucl. Phys. **B190**, 692 (1981).
[3] A. Di Giacomo and G. C. Rossi, Phys. Lett. **100B**, 481 (1981).
[4] J. Kripfganz, Phys. Lett. **101B**, 169 (1981); R. Kirschner, J. Kripfganz, J. Ranft, and A. Schiller, Nucl. Phys. **B210**, 567 (1982).
[5] E.-M. Ilgenfritz and M. Müller-Preussker, Phys. Lett. **119B**, 395 (1982).
[6] R. Alfieri, F. Di Renzo, E. Onofri, and L. Scorzato, Nucl. Phys. **B578**, 383 (2000).
[7] F. Di Renzo and L. Scorzato, J. High Energy Phys. 10 (2001) 038.
[8] P. E. L. Rakow, Proc. Sci., LAT2005 (2006) 284.
[9] Y. Meurice, Phys. Rev. D **74**, 096005 (2006).
[10] J. C. LeGuillou and J. Zinn-Justin, *Large-Order Behavior of Perturbation Theory* (North-Holland, Amsterdam, 1990).
[11] S. Narison and V. I. Zakharov, Phys. Lett. B **679**, 355 (2009).
[12] E.-M. Ilgenfritz, Y. Nakamura, H. Perlt, P. E. L. Rakow, G. Schierholz, and A. Schiller, Proc. Sci., LAT2009 (**2009**) 236.
[13] R. Horsley, G. Hotzel, E.-M. Ilgenfritz, Y. Nakamura, H. Perlt, P. E. L. Rakow, G. Schierholz, and A. Schiller, Proc. Sci., LATTICE2010 (**2010**) 264.
[14] G. Parisi and Y.-s. Wu, Sci. Sin., Ser. A, Math. phys. astron. tech. sci. **24**, 483 (1981).
[15] F. Di Renzo and L. Scorzato, J. High Energy Phys. 10 (2004) 073.
[16] G. Bali (private communication).
[17] U. M. Heller and F. Karsch, Nucl. Phys. **B251**, 254 (1985).
[18] R. Horsley, P. E. L. Rakow, and G. Schierholz, Nucl. Phys. B, Proc. Suppl. **106**, 870 (2002).
[19] C. Domb and M. F. Sykes, Proc. R. Soc. A **240**, 214 (1957).
[20] G. P. Lepage and P. B. Mackenzie, Phys. Rev. D **48**, 2250 (1993).
[21] R. Wohlert, P. Weisz, and W. Wetzel, Nucl. Phys. **B259**, 85 (1985).
[22] B. Alles, A. Feo, and H. Panagopoulos, Phys. Lett. B **426**, 361 (1998); **553**, 337(E) (2003).

[23] A. Athenodorou, H. Panagopoulos, and A. Tsapalis, Nucl. Phys. B, Proc. Suppl. **140**, 794 (2005).
[24] F. Di Renzo, G. Marchesini, and E. Onofri, Nucl. Phys. **B497**, 435 (1997).
[25] G. Martinelli and C. T. Sachrajda, Nucl. Phys. **B478**, 660 (1996).
[26] See, e.g., M. Beneke, Phys. Rep. **317**, 1 (1999).
[27] I. M. Suslov, Zh. Eksp. Teor. Fiz. **127**, 1350 (2005); J. Exp. Theor. Phys. **100**, 1188 (2005).
[28] V. Zakharov, Nucl. Phys. B, Proc. Suppl. **207–208**, 306 (2010).
[29] E.-M. Ilgenfritz, H. Perlt, and A. Schiller (unpublished).
[30] G. Burgio, F. Di Renzo, G. Marchesini, and E. Onofri, Phys. Lett. B **422**, 219 (1998).
[31] S. Necco and R. Sommer, Nucl. Phys. **B622**, 328 (2002).
[32] M. A. Shifman, Nucl. Phys. **B173**, 13 (1980).
[33] S. Narison, Phys. Lett. B **387**, 162 (1996).
[34] C. Bauer, G. S. Bali, and A. Pineda, Phys. Rev. Lett. **108**, 242002 (2012).
[35] M. E. Luke, A. V. Manohar, and M. J. Savage, Phys. Rev. D **51**, 4924 (1995).
[36] I. I. Kogan and M. A. Shifman, Phys. Rev. Lett. **75**, 2085 (1995).
[37] A. Patrascioiu, E. Seiler, and I. O. Stamatescu, Phys. Lett. **107B**, 364 (1981).
[38] E. Seiler, I. O. Stamatescu, and D. Zwanziger, Nucl. Phys. **B239**, 177 (1984).